SESSION 3

Chairman: Dr. P. WYDLER (Switzerland)

FEASIBILITY STUDIES ON MA AND FP TRANSMUTATION IN FAST REACTORS

T.Wakabayashi and N.Higano

Oarai Engineering Center
Power Reactor and Nuclear Fuel Development Corporation

Abstract

Feasibility studies have been performed to develop an optimized fast reactor core for reducing long-term radiotoxicity of nuclear waste by minor actinide(MA) and long-lived fission product(FP) transmutation , taking into consideration fuel cycle technology. Systematic parameter survey calculations were implemented to investigate the basic characteristics of MA and FP transmutation in a fast reactor core . The hybrid MA-loading method , where Np nuclide is dispersed uniformly in the core and target subassemblies containing Am, Cm and rare earth nuclides are loaded into the blanket region , has the potential to achieve the maximum transmutation of MA with no special fuel design considerations. The introduction of target subassemblies using duplex pellets - a moderator annulus surrounding a ^{99}Tc core - has a great potential to transmute long-lived fission products in the radial blanket region of the fast reactor core .

1. INTRODUCTION

One of the distinctive features of a fast reactor is its good neutron economy. Utilizing the excess of neutrons enables us to construct flexible cores such that they breed or burn plutonium in consideration of plutonium stockpile balance, and also incinerate minor actinides(MA) and long-lived fission products to reduce radiotoxicity.

Some of the MA nuclides (Np,Am,Cm) and fission products(^{99}Tc,^{129}I etc.) contained in residual waste from reprocessing have extremely long-term radiotoxicity. Partitioning and transmutation of the MA and fission products are attracting considerable attention at present as an option to reduce the long-term radiological hazard of the high-level nuclear waste. There is general agreement that the implementation of partitioning and transmutation in waste management is technically feasible.

Means of reducing the radiotoxicity of the MA nuclides are presently under investigation. The MA nuclides could produce useful energy if converted into short-lived fission products by neutron bombardment. From this standpoint, a nuclear reactor provides the obvious means for transmutation of MA nuclides. Among the various nuclear reactors, a fast reactor is considered to have the greatest potential to transmute MA effectively , because of its hard neutron spectrum(1)-(5).

The beta-emitting fission products technetium(^{99}Tc, half-life 2.13x10^5 year) and iodine(^{129}I, half-life 1.57x107 year) are among the important long-lived nuclides in high-level waste, they dominate the beta radiotoxicity for more than a million years. Transmutation of ^{99}Tc and ^{129}I by neutron capture as a result of irradiation in nuclear reactors will yield the stable isotopes ^{100}Ru and ^{130}Xe, respectively. However, due to the small neutron cross sections , the transmutation efficiency in LWRs is low. Moderated subassemblies in fast reactors are more appropriate devices for the transmutation of the fission products.

Feasibility studies have been performed to investigate the basic transmutation characteristics of MA and long- lived fission products in the fast reactor(6,7).

2. MA Transmutation

Systematic parameter survey calculations were implemented to investigate the basic characteristics (transmutation rate , burnup reactivity, Doppler coefficient, sodium void reactivity , maximum linear heat rate, etc.) of a fast reactor core with MA transmutation, the following items were considered:

(1)Study on loading method of MA in the core (homogeneous , heterogeneous , hybrid , blanket, etc.)

(2)Selection of fuel material for MA transmutation (oxide ,inert matrices such as Al_2O_3 , CeO_2 , etc.),

(3)Study on the maximum tolerable amount of rare earth (RE) nuclides ,

(4)Effect of MA recycling on core characteristics and fuel cycle system.

(1) Study on MA Loading method

Since MA loading considerably affects not only core characteristics but also fuel material properties, it is necessary to investigate MA loading methods taking into account this influence upon

core characteristics and fuel material properties. Possible MA loading methods (homogeneous , heterogeneous , hybrid , blanket , etc.) were investigated for fast reactor cores with no special design adaptation for MA loading. The MA is dispersed uniformly throughout all the fuel in the core in the homogeneous method . In the heterogeneous method , a small number of fuel subassemblies with concentrated MA (target S/As) are loaded into the core. The hybrid MA loading method is a combination of the homogeneous and heterogeneous methods : the Np nuclide is loaded in the core region uniformly and a small number of subassemblies containing Am ,Cm and RE nuclides are loaded into the blanket region.

The comparison of core performance for various MA loading methods is shown in Table 1. The MA transmutation in a fast reactor core has no serious drawbacks in terms of core performance, provided that the homogeneous loading method can be employed with a small ratio of MA to fuel (~5wt%). Since a 1000MWe-class LWR produces about 26 kg of MA per year, a fast reactor with 5%wt MA loading can transmute the MA mass from six LWRs .

The heterogeneous MA loading method can be made feasible by optimizing the fuel design, loading pattern and the coolant flow of the MA-loaded fuel subassemblies. The reduction of the fuel pin diameter and the Pu enrichment is essential to reduce the power of MA-loaded fuel in the heterogeneous MA loading method.

The hybrid MA loading method can transmute a large amount of MA without serious drawbacks in terms of core performance. The transmuted mass of MA is about 530kg/cycle, which is almost 16 times the mass produced by an LWR of the same power output.

The MA loading in the blanket region causes no problems from the viewpoint of core performance. Minor actinides are transmuted at a rate of 6% per cycle in the axial and radial blanket regions.

It was found that the hybrid MA loading method , where the Np nuclide is dispersed uniformly in the core and target subassemblies containing Am, Cm and rare earth nuclides are loaded into the blanket region , has the potential to achieve the maximum transmutation of MA with no special design considerations.

(2)Selection of fuel material for MA transmutation

Different types of inert matrices , instead of UO_2 , for the heterogeneous MA-loading method have been investigated , they avoid the buildup of higher actinides via ^{238}U and achieve a high MA transmutation rate. Inert matrices of Al_2O_3 and CeO_2 were examined in this study. The MA transmutation rate of the target subassembly using inert matrices is larger than that of the target subassembly using UO_2 . The use of inert matrices in the target subassembly effectively increases the MA transmutation rate.

(3) Study on the permissible RE level in homogeneously loaded MA

Systematic parameter survey calculations were performed to investigate the basic characteristics of a fast reactor core loaded homogeneously with MA which contains RE , and also to establish a MA and RE loading method which has no serious influence on the core design. The homogeneous loading of MA and RE has no serious effects on the reactor core performance , provided that the amounts of MA and RE in the fuel are less than 5 and 10wt% respectively . In the case of adding Am,Cm and RE in the radial blanket region , it is possible ,

from the viewpoint of core performance , to insert ~50wt% of Am and Cm, and ~50wt% of RE in the target assemblies , as is shown in Table 1.

(4)Effect of MA recycling on core characteristics and fuel cycle system.

The effects of MA recycling on the core characteristics and the fuel cycle system in the homogeneous loading method were evaluated . The absolute value of the Doppler coefficient is increased by MA recycling , the value at the 8th recycle is ~14% larger in comparison with that in the initial core , as is shown in Table 2 . This is caused by the reduction in Pu enrichment with MA recycling , this increases the resonance absorption of ^{238}U. Sodium void reactivity decreases with MA recycling , and the value at the 8th recycle is ~7% smaller than that in the initial core. The recycling of MA in a fast reactor is feasible from neutronic and thermal-hydraulic points of view . However, during multi-recycling the Np fraction is significantly reduced compared to the unirradiated feed, and the fraction of Cm is greatly increased because of neutron capture in Am. The accumulation of Cm as a result of the MA recycling will bring about some problems concerning fuel handling and reprocessing , because of an increase in both the decay heat and the neutron emission rate from ^{244}Cm .

3. FP Transmutation

To calculate the transmutation rate of ^{99}Tc in a neutron flux spectrum it is insufficient to account for the thermal neutron capture only ; the epithermal part of the neutron spectrum also has a contribution. There is a large resonance peak at 5.6eV and a series of minor resonances between 10 and 100eV. This suggests that a neutron spectrum where there is more absorption in the resonance region than in the thermal region is advantageous in order to increase the absorption rate of ^{99}Tc. This is because such a spectrum helps to suppress absorption by structural materials. Therefore , the appropriate loading mass of moderator depends upon its moderating power.

Systematic parameter survey calculations were performed to investigate the basic characteristics of FP(^{99}Tc) transmutation in the blanket region of a fast reactor. A moderated target subassembly was used for ^{99}Tc transmutation. The subassembly consists of moderator pins containing $ZrH_{1.7}$ and ^{99}Tc target pins distributed between the moderator pins. The moderated target subassemblies were loaded in the radial blanket region of the fast reactor core. The arrangement of the moderator and the target pins in the subassembly , the volume ratio of target to moderator and the moderator materials were selected as parameters in the present study. A new concept of duplex pellet - a moderator annulus surrounding a ^{99}Tc core - for ^{99}Tc transmutation was also adopted in the present study to get a better transmutation performance.

The core configuration and main parameters of the 600MWe-class fast reactor core used in the study are shown in Fig. 1. The arrangements of the moderator pins and the FP pins in the subassembly are shown in Fig. 2. The Monte Carlo computer code for neutron photon transport (MVP)[8] was adopted for FP transmutation calculations in the moderated target subassembly because of its versatility and comprehensive geometry features.

The dependence of ^{99}Tc transmutation performance on the number of FP pins in the 127-pin target assembly is shown in Table 3. The transmutation rate of ^{99}Tc increases as the

number of FP pins in the target subassembly decreases , because the moderating power increases.

The sensitivity of the ^{99}Tc transmutation performance to the neutron spectrum in the target subassemblies was calculated by changing the moderator materials($ZrH_{1.7}$, BeO , Al_2O_3 , SiC). Table 4 shows the results of ^{99}Tc transmutation performance for various moderator materials. Neutron spectra and capture reaction rate distributions of ^{99}Tc in the FP pin region for various moderator materials are shown in Fig. 3 and 4 , respectively. It was found that the moderating power of $ZrH_{1.7}$ and of BeO is better than that of Al_2O_3 or SiC for ^{99}Tc transmutation.

The FP transmutation performance of a new target subassembly concept using duplex pellets consisted of ^{99}Tc and $ZrH_{1.7}$ was investigated. Configurations of moderated target subassemblies using duplex pellets are shown in Fig. 5. The results of the calculations are shown in Table 5. The transmutation rate of ^{99}Tc in the new target subassembly is larger than that in the subassembly consisting of separate $ZrH_{1.7}$ moderator pins and ^{99}Tc target pins as shown in Fig. 2. As a result of the present study , a maximum ^{99}Tc transmutation rate of about 10%/year was obtained by using the new target subassembly loaded in the blanket region of the fast reactor . The new target subassembly can achieve the optimum transmutation performance by adjusting the volume ratio of $ZrH_{1.7}$ and ^{99}Tc in the duplex pellet.

The effects of loading target subassemblies on main core characteristics were also analyzed. It was found that the power density of the core fuel adjacent to the target is rather high and is about the same as the maximum in the core. However , the power spike is much mitigated compared to the case of loading target subassemblies in the core region.

4. CONCLUSION

Feasibility studies have been performed to investigate the basic characteristics of MA and FP transmutation in fast reactors , and also to clarify the feasibility of MA and FP transmutation .

MA transmutation in a fast reactor core has no serious drawbacks in terms of core performance, provided that the homogeneous loading method can be employed with a small fraction of MA in the fuel (~5wt%). The hybrid MA-loading method , where Np nuclide is dispersed uniformly in the core and target subassemblies containing Am, Cm and rare earth nuclides are loaded into the blanket region , has the potential to achieve the maximum transmutation of MA with no special fuel design considerations.

The introduction of target subassemblies using duplex pellets - a moderator annulus surrounding a ^{99}Tc core - gives the maximum transmutation rate of Tc-99 in the radial blanket region of the fast reactor core.

It was found that the fast reactors have an excellent potential for transmutating MA and FP effectively. However, much research needs still to be done to improve the partitioning of the radionuclides as well as to resolve the technological problems of the transmutation, to make the process industrially attractive.

REFERENCES

(1)M. YAMAOKA ,M. ISHIKAWA and T. WAKABAYASHI, "Feasibility Study of TRU Transmutation

by LMFBRs", Proc. Int. Conf. on Fast Reactors and Related Fuel Cycles (FR'91),Vol. IV, Oct., 28-Nov. 1 , Kyoto (1991).
(2)T. WAKABAYASHI ,M. YAMAOKA , M. ISHIKAWA and K. HIRAO, "Status of Study on TRU Transmutation in LMFBRs", Trans. Am. Nucl. Soc., 64, 556 (1991).
(3)M. YAMAOKA and T. WAKABAYASHI, "Design Study of A Super Long Life Core Loaded with TRU Fuel", Proc. Int. Conf. on Design and Safety of Advanced Nuclear Power Plants (ANP'92),Vol. I, October 25-29, Tokyo (1992).
(4)T. WAKABAYASHI and T. IKEGAMI, "Characteristics of an LMFBR Core Loaded with Minor Actinide and Rare Earth Containing Fuels", Proc. Int. Conf. on Future Nuclear Systems : Emerging Fuel Cycles and Waste Disposal Options (GLOBAL'93),Vol. I, Sep. 12-17 , Seattle (1993)
(5)T.WAKABAYASHI, S.OHKI, T.IKEGAMI ,"Feasibility studies of an optimized fast reactor core for MA and FP transmutation", Proc. Int. Conf. on Evaluation of Emerging Nuclear Fuel Cycle Systems (GLOBAL'95),Vol. I, Sep. 11-14 , Versailles, France (1995.)
(6)D.W. WOOTAN and J.V.NELSON, "Transmutation of Selected Fission Products in a Fast Reactor", Proc. Int. Conf. on Future Nuclear Systems : Emerging Fuel Cycles and Waste Disposal Options (GLOBAL'93),Vol. II, Sep. 12-17 , Seattle (1993).
(7)J.TOMMASI, M. DELPECH , J.P.GROUILLER and A. ZAETTA, "Long-Lived Waste Transmutation in Reactors", Proc. Int. Conf. on Future Nuclear Systems : Emerging Fuel Cycles and Waste Disposal Options (GLOBAL'93),Vol. II, Sep. 12-17 , Seattle (1993).
(8)M.NAKAGAWA and T.MORI , J. Nucl. Sci. Technol., 30(7),692 (1993).

Table 1 Comparison of Core Performance for Various Ma Loading Methods

Item	Reference (No MA)	Homo. Loading	Hetero. Loading	Homo. Loading	Hybrid Loading	Hybrid Loading
MA and RE Loaded in the Core Region	-	Np,Am,Cm :5% RE : 0%	Np,Am,Cm :49% RE : 0% (Number of target S/A:39)	Np,Am,Cm :5% RE : 10%	Np : 9.8% RE : 0%	Np : 9.8% RE : 0%
MA and RE Loaded in the Blanket Region(Target)	-	-	-	-	Am,Cm: 46% RE : 46% (Number of target S/A:72)	Am,Cm: 46% RE : 46% (Number of target S/A:72)
Matrix of Target			UO_2		UO_2	Al_2O_3
Pu Enrichment (wt%)(IC/OC)	15.4 /18.6	16.6 /20.1	15.4 /18.6	20.0 24.2	19.0 23.4	19.0 23.4
Burnup Reactivity (%Δk/kk')	3.31	2.12	1.83	3.71	0.87	0.90
Max.Linear Heat Rate(w/cm) (Driver/Target)	420	407	439 /309	413	405 /217	406 /174
Na Void Reactivity	1.0	1.3*	1.3*	1.4*	1.5*	1.5*
Doppler Coefficient		0.6*	0.7*	0.5*	0.45*	0.45*
MA Tran						
Amount(kg/cycle)	-	172	186	164	514	529
Rate(Core)(%/cycle)	-	10.9	11.3	10.3	13.9	14.0
Rate(Blanket) (%/cycle)	-	-	-	-	2.9	3.3

* Relative Value

Table 2 Effect of MA Recycling on Core Performance (Homogeneous Loading Method)

Item	Reference (InitialCore)	4th Recycle	8th Recycle
MA(wt%)	5	5	5
Pu Enrichment (wt%)	17.8(Inner) 21.6(Outer)	17.6(Inner) 21.3(Outer)	16.9(Inner) 20.4(Outer)
Burnup Reactivity (%Δk/kk')	1.6	0.4	0.5
Na Void Reactivity	1.0 (Ref.)	0.96 (Relative Value)	0.93 (Relative Value)
Doppler Coefficient	1.0 (Ref.)	1.08 (Relative Value)	1.14 (Relative Value)
MA Transmutation Rate(%)	10.3	10.5	10.1

Table 3 Dependence of ^{99}Tc transmutation performance on the number of FP pins in the 127-pin target assembly.

No.of FP pins	Radius of FP pins (cm)	V_{fp}/V_{mod}	Transmutation Rate (%/y)	Transmuted ^{99}Tc amounts(kg/y)	Loaded ^{99}Tc amounts (kg)
52	0.5	0.69	1.5	47.0	3170
37	0.5	0.41	1.8	41.1	2250
27	0.5	0.27	2.1	34.4	1640
22	0.5	0.17	2.5	27.2	1100

Table 4 Difference of ^{99}Tc transmutation performance on moderator material

Moderator	Transmutation Rate(%/y)	Transmuted FP amounts(kg/y)
$ZrH_{1.7}$	2.1	34.4
BeO	2.2	36.0
Al_2O_3	1.7	28.0
SiC	1.6	27.0

Table 5 Results of parameter survey calculations on ^{99}Tc transmutation performance using duplex moderator pins.

No.of duplex pins	FP pin Radius (mm)	Transmutation Rate (%/y)	Transmuted amounts(kg/y)	Loaded amounts(kg)
127	2.00	3.5	38.1	1101
127	0.63	9.8	10.8	110
217	2.00	2.5	46.7	1882
217	0.63	9.1	17.1	188
37	5.30	1.9	41.8	2253
37	0.63	10.1	2.9	29

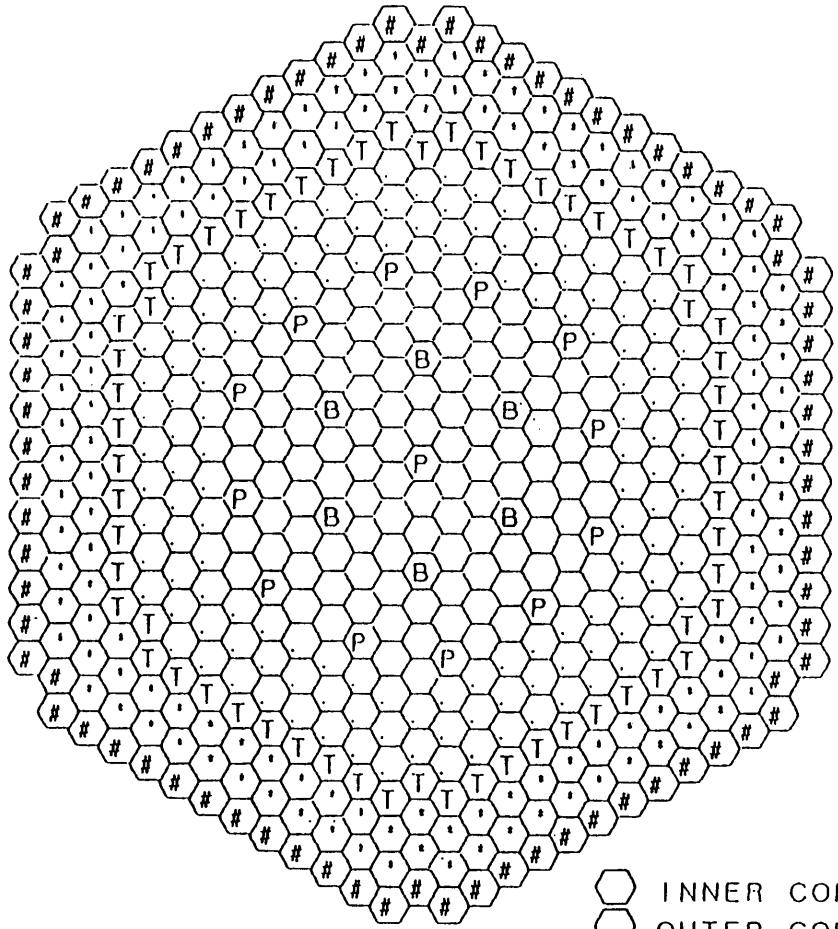

INNER CORE	108
OUTER CORE	138
PRIMARY CR	13
BACKUP CR	6
TARGET ASSEMBLY	60
SUS SHIELD	138
B4C SHIELD	78

Reactor Power	1600MWth
Core Height	100cm
Axial branket	35cm
Core Diameter	275m
Fuel Type	MOX
Pu Enrichment	15.30/18.90
Pu composition 8/9/0/1/2	3/53/25/12/7
Core Pitch	160.7mm

Volume Fraction

	Fuel	Gap	SUS	Sodium	Absober
Core	38.2	5.1	22.4	34.3	-
PCR	-	5.2	15.6	45.6	33.6
BCR	-	5.2	15.6	15.6	33.6
Shielding	-	-	80.0	20.0	

Fig. 1 Core layout and main parameters

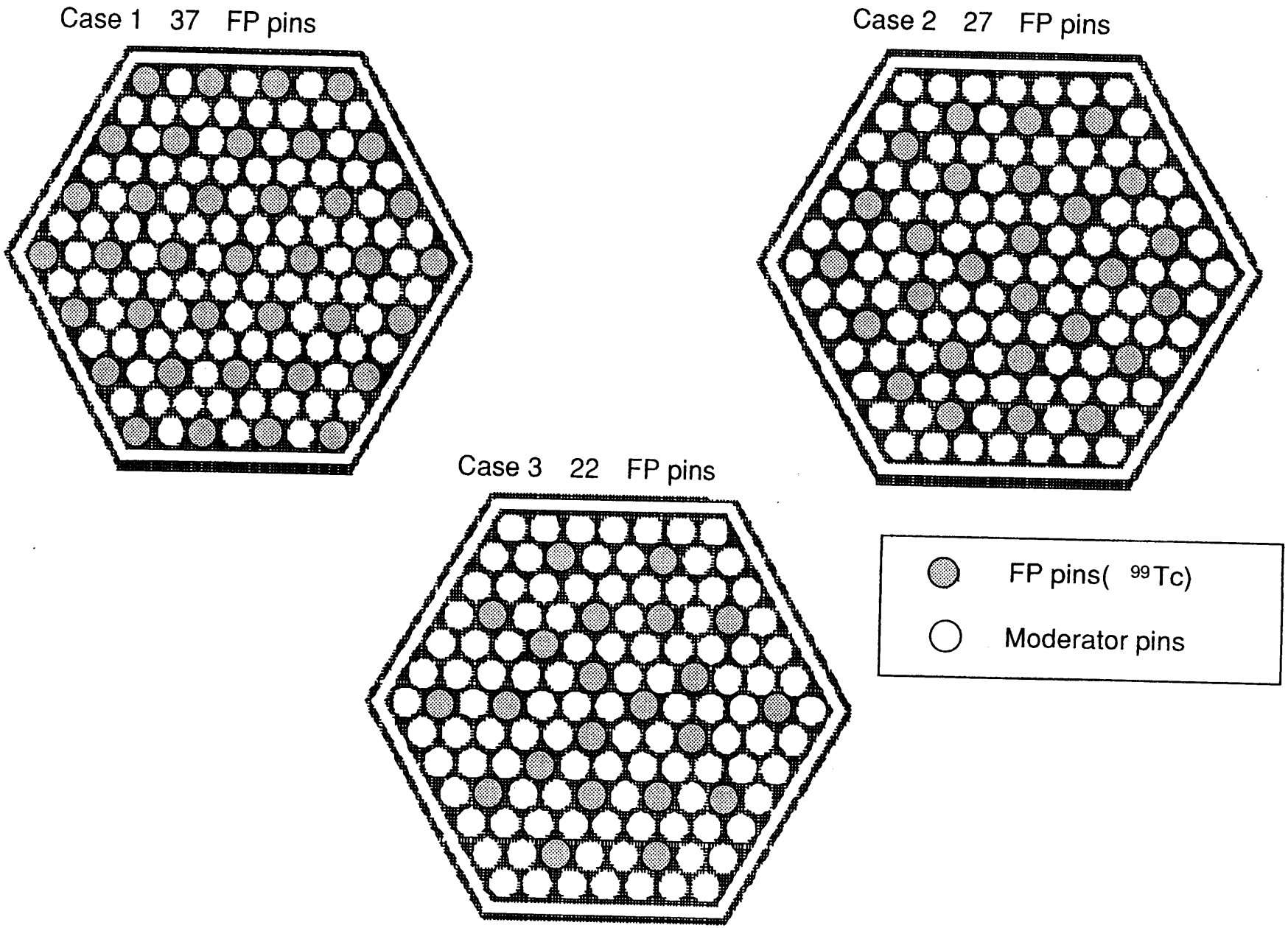

Fig.2 ^{99}Tc pin arrangements in Target Assembly (based on 127-pin assembly)

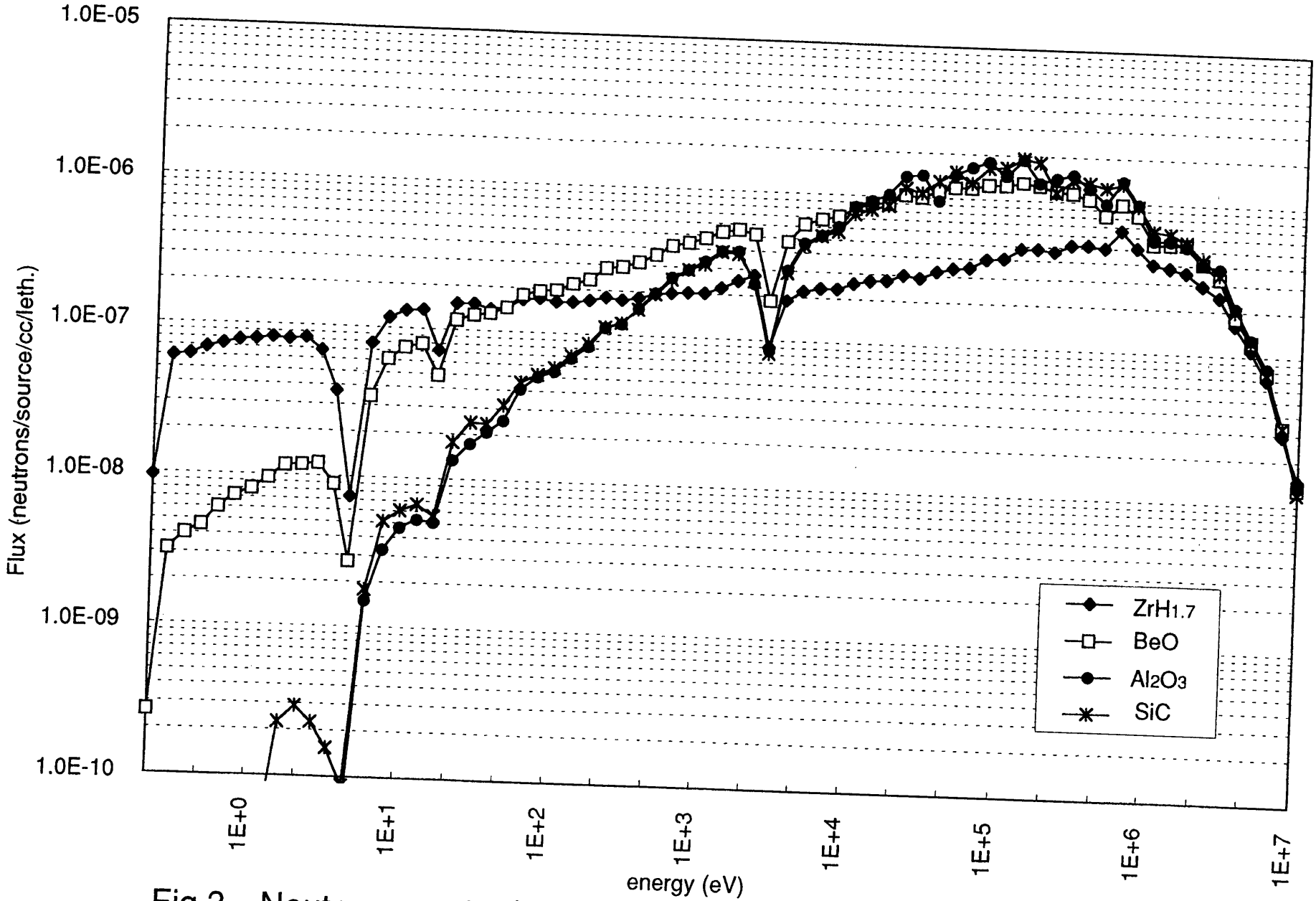

Fig.3 Neutron spectra in ^{99}Tc region for various moderator materials (27 FP pins in 127 pins model)

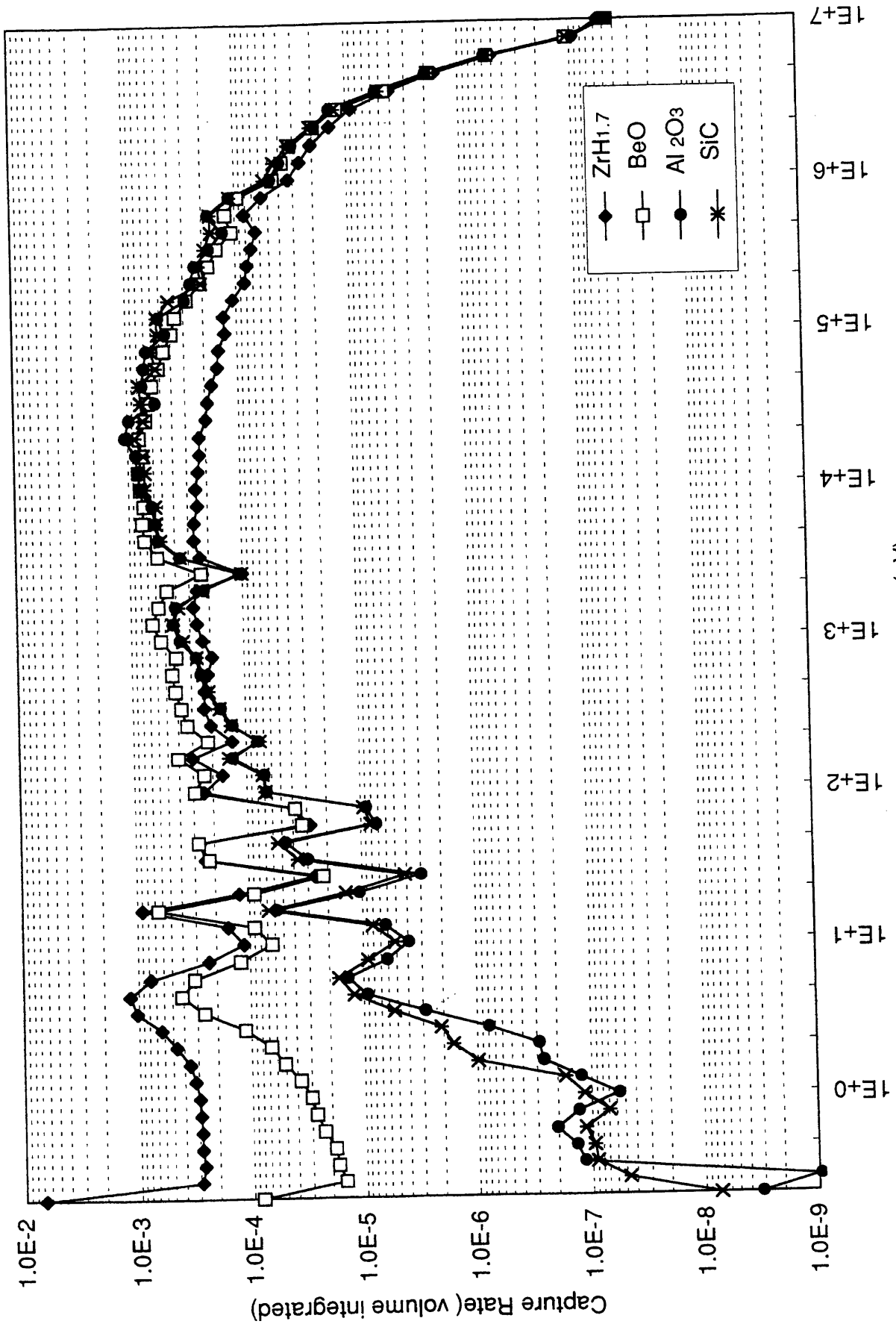

Fig. 4 Capture Rates in ^{99}Tc region for varions moderator materials
(27 FP pins in 127 pins model)

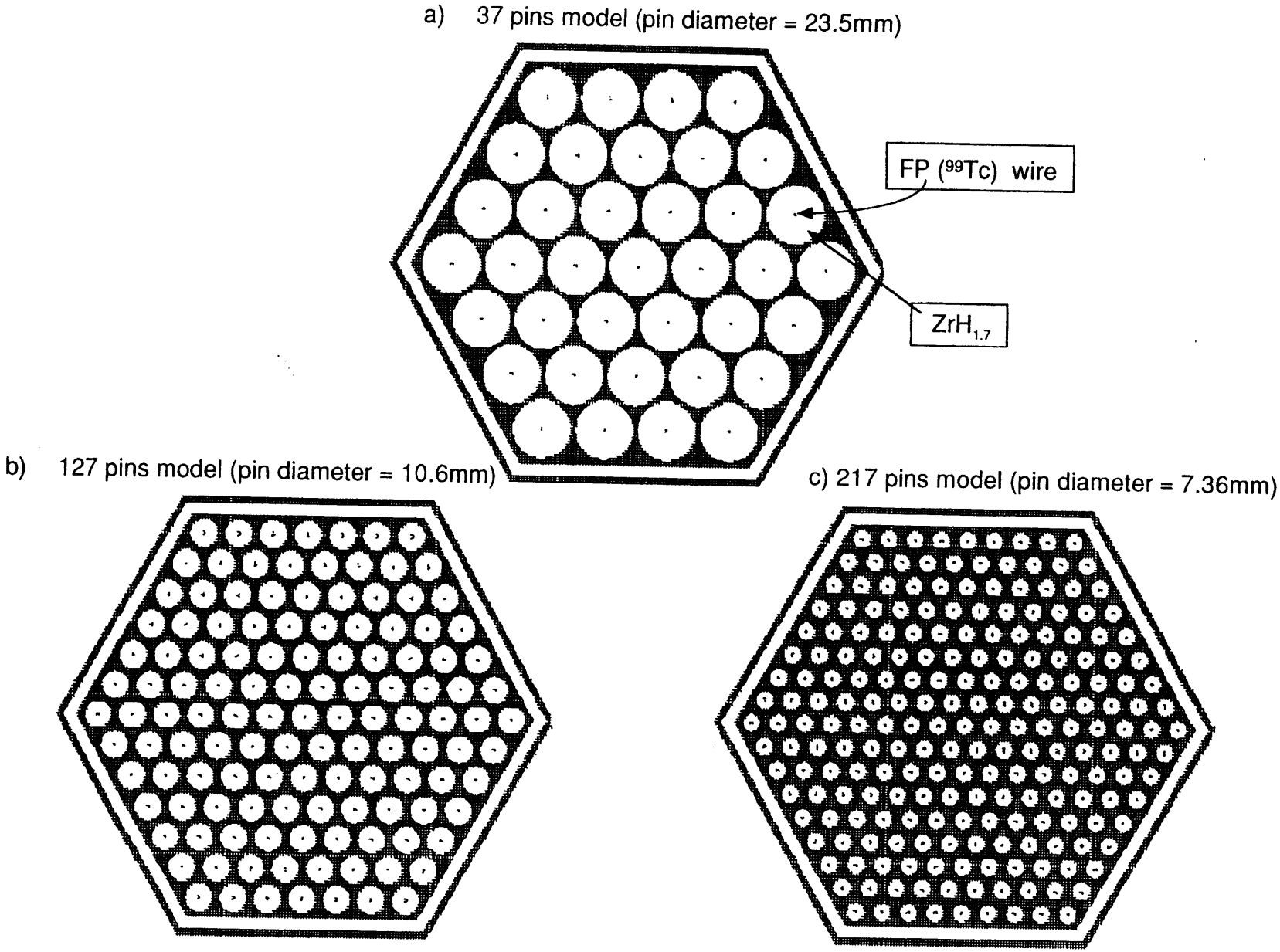

Fig. 5 Duplex pin arrangements in Target assembly (Radius of FP(^{99}Tc)= 0.6mm or 2.0mm)

TRANSMUTATION OF TECHNETIUM IN THE PETTEN HFR: A COMPARISON OF MEASUREMENTS AND CALCULATIONS

J.L. Kloosterman, J.A. Hendriks and R.J.M. Konings
Netherlands Energy Research Foundation (ECN)
P.O. Box 1, NL-1755 ZG Petten, Netherlands
Tel: ++31 224 564402, Fax: ++31 224 563490
E-mail: kloosterman@ecn.nl

Abstract

Within the framework of the EFTTRA cooperation between CEA, ECN, EDF, FZK, IAM and ITU, six metallic ^{99}Tc rods have been irradiated in the Petten HFR for 193 effective full power days. During this irradiation, more than 6% of the ^{99}Tc has been transmuted to the stable ^{100}Ru. At ECN, one of the six rods has been examined in the hot cell laboratory. The ruthenium concentration in the rod measured by Isotope Dilution Mass Spectrometry reaches 6.4% at 5 mm from the bottom of the rod and 6.0% at 5 mm from the top. Also the axial and radial distributions of the ruthenium have been measured by Electron Probe Micro Analysis. The ruthenium concentrations calculated by the three-dimensional Monte Carlo code KENO reach 6.1% at 5 mm from the bottom of the rod and 5.7% at 5 mm from the top. These values are in reasonable agreement with the measured ones. However, the calculated radial distribution of the ruthenium concentration is not in agreement with the measurements. The radial profile calculated by the Monte Carlo code MCNP, which uses a point-wise cross-section library, agrees much better with the measurements.

To solve the remaining small differences between the measured and calculated ruthenium concentratrions in the rod, the thermal absorption cross section of ^{99}Tc will be measured in the Petten HFR in the course of this year.

1 Introduction

The long-lived fission products ^{99}Tc and ^{129}I are among the most important nuclides that dominate the beta activity of spent fuel after a hundred thousands of years. Because of their high solubility in (ground)water, technetium and iodine are easily transported to the biosphere once they are released from the deep-geological waste repository. To reduce the dose risks to future generations, technetium and iodine should be partitioned from the spent fuel and treated separately, e.g. transmuted in nuclear reactors or conditioned by chemical immobilization.

In 1992, the EFTTRA collaboration (Experimental Feasibility of Targets for TRAnsmutation) was founded between CEA, ECN, EDF, FZK, IAM and ITU, with the aim to investigate experimentally the behaviour of targets during irradiation in fast and thermal nuclear reactors and to demonstrate the applicability of scenarios for the transmutation of long-lived fission products and minor actinides [1].

This paper describes the irradiation and the results of the Post Irradiation Examinations (PIE) of one ^{99}Tc rod irradiated in the Petten thermal High Flux Reactor (HFR) within the framework of the EFTTRA cooperation. During the irradiation, the long-lived ^{99}Tc is transmuted to the stable ^{100}Ru. The measured ruthenium concentration and profiles are compared with results of three-dimensional Monte-Carlo calculations.

2 Target fabrication and Irradiation

Six metallic technetium rods of 4.8 mm diameter and 25 mm length were fabricated by ITU in Karlsruhe. Details of the fabrication method are described in reference [2]. The specific density was higher than 99.9% of the theoretical density. Analysis by glow-discharge mass spectrometry showed that the ruthenium concentration in the metal was less than 1 ppm. The rods were enclosed in stainless steel capsules (Phenix cladding material), provided by CEA. Each capsule contained two rods on top of each other.

The targets were positioned in peripheral holes of an aluminium sample holder. Three holes were occupied by the six ^{99}Tc rods (two rods on top of each other) and the other six holes were filled by iodine targets. The sample holder was placed in an aluminium filler element and loaded in the core position C5 of the Petten HFR. At this position, the total neuton flux in the targets exceeds 10^{15} $cm^{-2}s^{-1}$ with a thermal component higher than 2 10^{14} $cm^{-2}s^{-1}$. Close to the technetium and iodine targets, fluence detectors (^{59}Co and ^{56}Fe) and gamma scan wires were located to monitor the thermal and fast neutron fluences. Also nine thermocouples were installed to measure the temperature of the facility. The geometry of the irradiation facility is shown in figure 1.

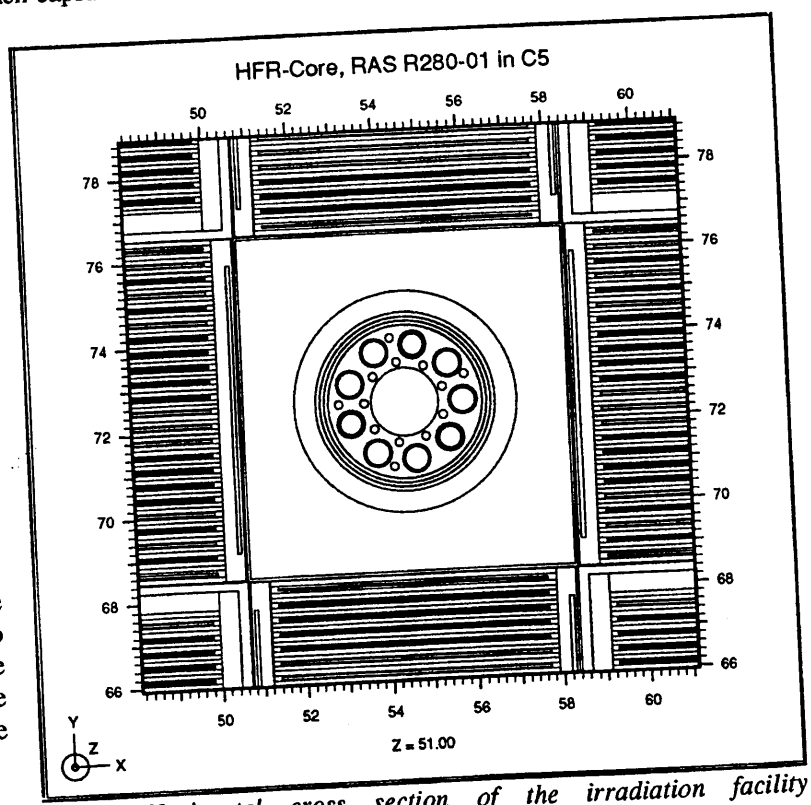

Fig. 1: *Horizontal cross section of the irradiation facility surrounded by HFR fuel assemblies.*

The irradiation lasted for eight cycles (192.95 effective full power days in total) and ended at the beginning of 1995. Due to gamma heating, the temperature of the rods exceeded 900 K. At the end of the irradiation, the thermal neutron fluence (E<0.7 eV) averaged over the technetium rods has reached a value of 3 10^{21} cm^{-2} and the total neutron fluence a value of 2 10^{22} cm^{-2}.

3 Post Irradiation Examinations

A joint PIE programme has been defined by CEA, ITU and ECN for four rods, whereas the other two rods are being re-irradiated again in the Petten HFR to reach a transmutation level of 20%.

Visual inspection after the irradiation showed that almost no irradiation damage and no swelling has occured. Measurements by means of a micrometer and micrographic examinations confirmed these conclusions. Results of these measurements are given in table 1.

Table 1: *Dimensions of some technetium rods before and after the irradiation in the Petten HFR [2].*

^{99}Tc	Diameter (mm)		Length (mm)	
sample	pre-irr	post-irr	pre-irr	post-irr
A	4.80±0.01	4.83±0.01	25.05	25.09
B	4.81±0.02	4.84±0.01	25.05	25.12
D	4.81±0.02	4.83±0.03		

Electron Probe Micro Analysis (EPMA) has been used to measure the radial profiles of the ruthenium concentration at two intersections of rod D: one located at 5 mm from the bottom (section D1) and one at 5 mm from the top (section D2). These intersections are shown in figure 2. The EPMA method has also been used to measure the axial profile along the rod axis at intersection D3 (see figure 2). The absolute values of the ruthenium concentration at D1 and D2 have been measured by Isotope Dilution Mass Spectrometry (IDMS), which is expected to be more accurate for absolute measurements.

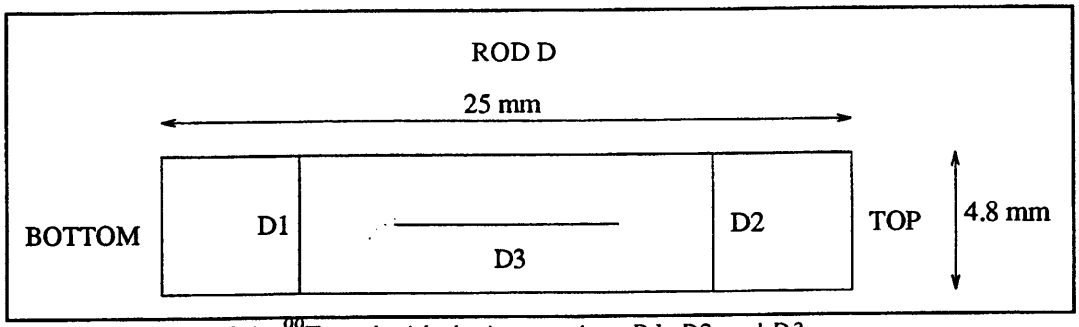

Fig. 2: *Drawing of the ^{99}Tc rod with the intersections D1, D2 and D3.*

The ruthenium concentration as a function of the cross-sectional area of the rod at intersection D1 is shown in figure 3. The two curves are the results of two measurements at different azimuthal angles perpendicular to each other. The vertical line at an area of 18.1 mm^2 denotes the outer edge of the rod with a diameter of 4.8 mm. The results at intersection D2 are very similar to the ones in figure 3 and shown in figure 4. In both figures, the so-called Rim effect caused by the resonance shielding of the neutrons is clearly visible. The difference between the profiles at the outer edge of the rod (area 18.1 mm^2) is most probably due to the position of the sample and the roughness of the surface of the rod.

The cross-sectional averaged ruthenium concentration measured by EPMA equals 7.2% at D1 and 6.8% at D2. However, as mentioned before, the EPMA method is not very accurate for absolute measurements. Therefore, two slices at each intersection D1 and D2 of the rod were dissolved in HNO_3 and the ruthenium concentration in each slice was measured several times by IDMS. The results are given in table 2.

Table 2: *Ruthenium concentrations at intersections D1 and D2 measured by Isotope Dilution Mass Spectrometry (IDMS).*

Slice	Ruthenium concentration (%)	
	D1	D2
1	6.39±0.15	5.98 ± 0.10
2	6.39±0.24	
Average	6.39±0.23	5.98 ± 0.10

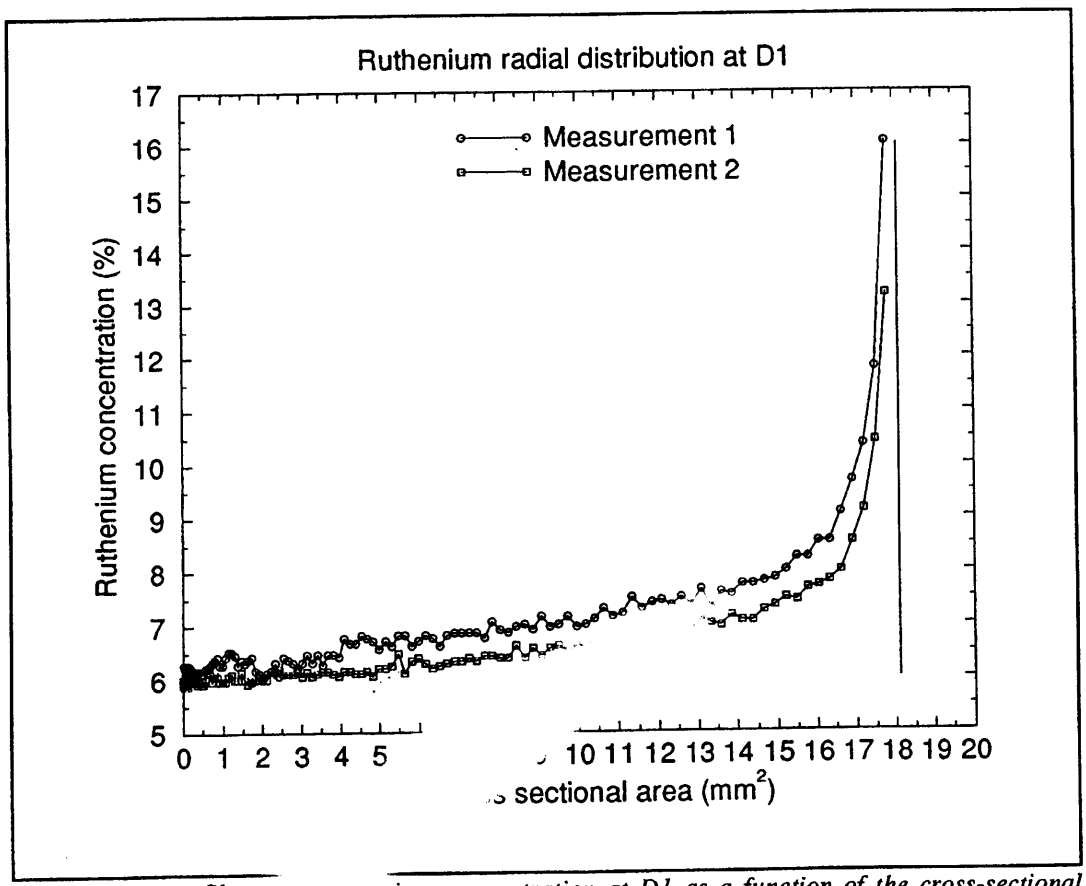

Fig. 3: *The profile of ruthenium concentration at D1 as a function of the cross-sectional area of the vertical line denotes the outer edge of the rod.*

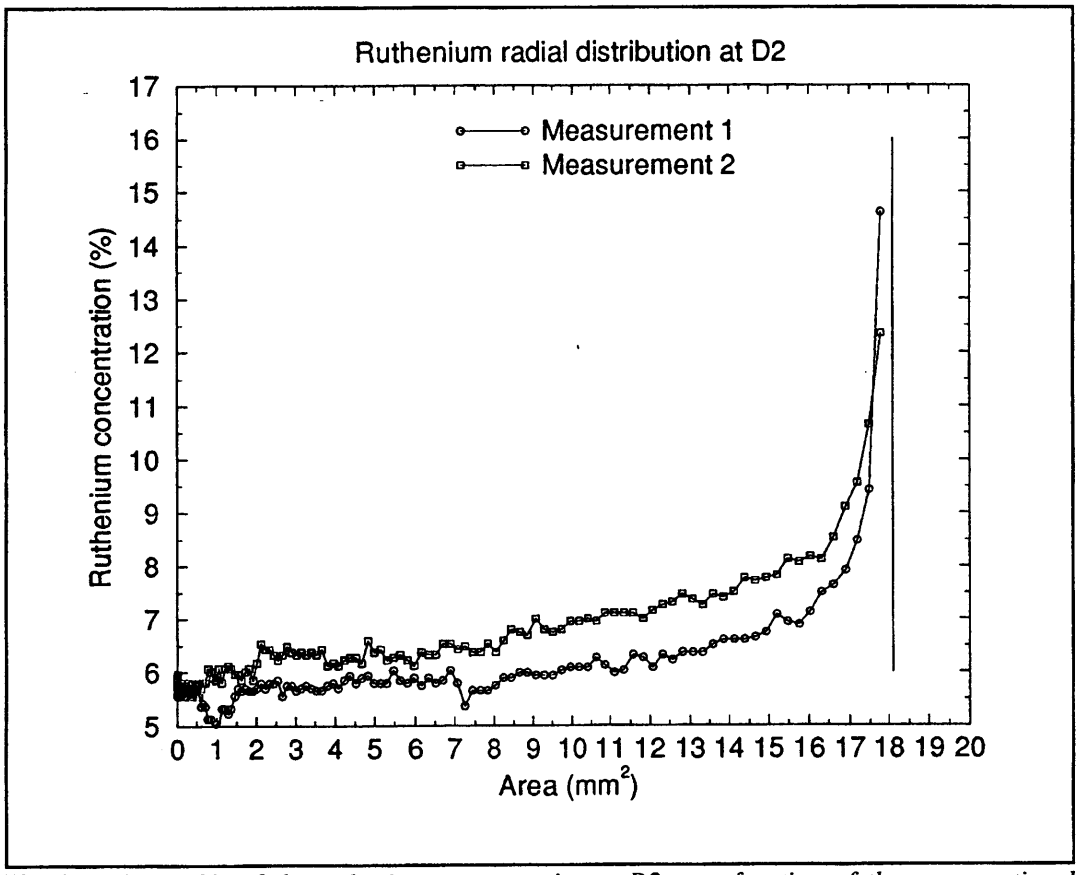

Fig. 4: *The profile of the ruthenium concentration at D2 as a function of the cross-sectional area of the rod. The vertical line denotes the outer edge of the rod.*

The ruthenium concentration at D3 as a function of the axial distance in the rod is shown in figure 5. The average ruthenium concentration is about 5.4%. Although there is a large spread in the results, the slope of the linear least squares fit indicates a small gradient of the ruthenium concentration as a function of the axial distance. According to this fit, the difference between the ruthenium concentrations at the intersections D1 and D2 along the rod axis would be 5.54-5.30=0.24%.

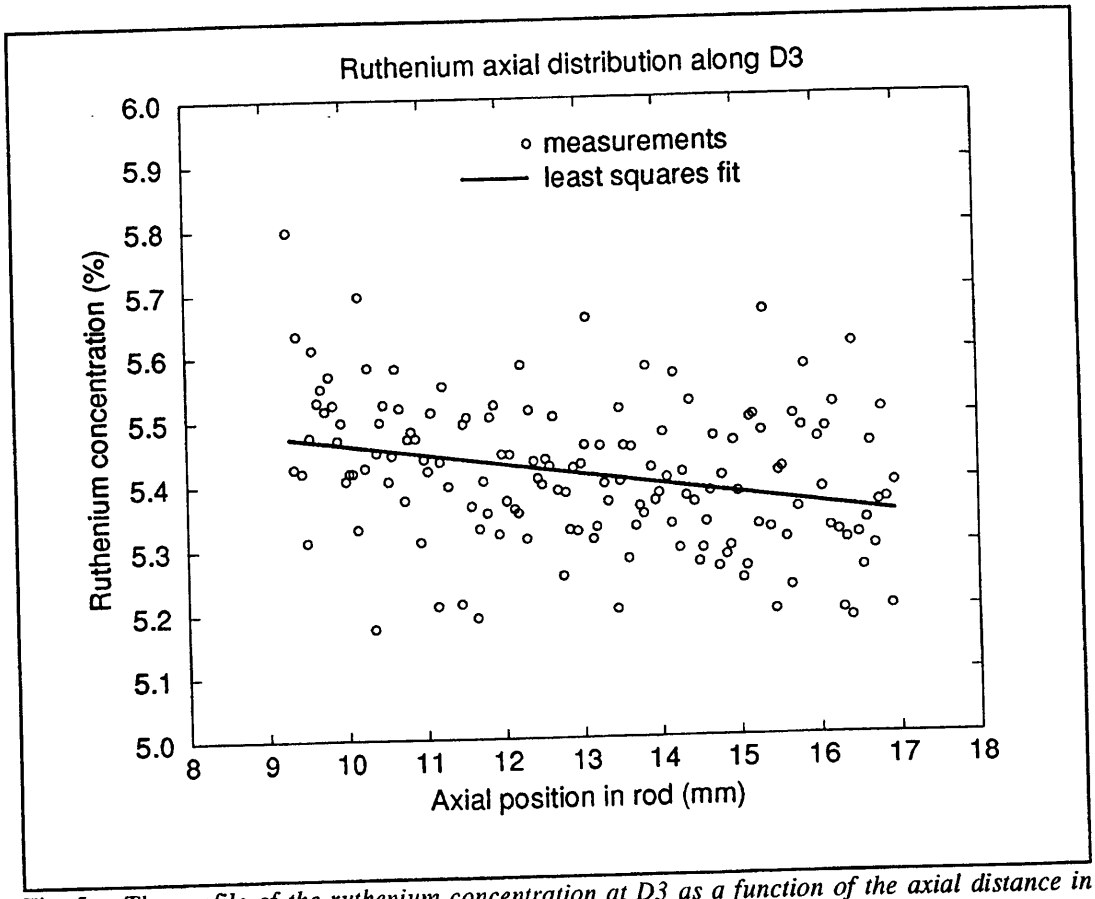

Fig. 5: *The profile of the ruthenium concentration at D3 as a function of the axial distance in the rod.*

4 KENO Monte Carlo Calculations

To assess the accuracy of the calculational methods and of the nuclear data files used in technetium transmutation studies, calculations have been performed by the Monte Carlo code KENO-Va [3] and associated nuclear data libraries based on the JEF2.2 evaluated file [4].

The standard three-dimensional core model of the Petten HFR has been used, which implies that the control members are at a fixed representative position and that a single type experimental facility was used to fill the experimental positions in the HFR model. This is done because it is too cumbersome to change the core model from one cycle to the other. The influence of these assumptions on the results is probably very small, because the experiment itself, which was loaded at position C5, has been modelled accurately, including the details on the fluence detectors (foils) and the gamma scan wires. Also the three-dimensional fuel distribution has been correctly represented. Figure 6 shows a horizontal cross section of the HFR core model with the experiment loaded at position C5, and figure 1 shows the irradiation facility in more detail.

In the calculations, the resonance shielding for all nuclides have been performed by the NITAWL-II code [5] (Nordheim method) in the resolved energy region and by the BONAMI-S code [6] (Bondarenko method) in the unresolved energy region, except for ^{99}Tc for which no resonance shielding in the unresolved region has been performed. This is due to the large background cross sections of ^{99}Tc in the unresolved region which may lead to negative cross sections when the resonance shielding is too large. Because the total contribution of the unresolved region to the capture rate is only 6.5%, this has no large effect on the results.

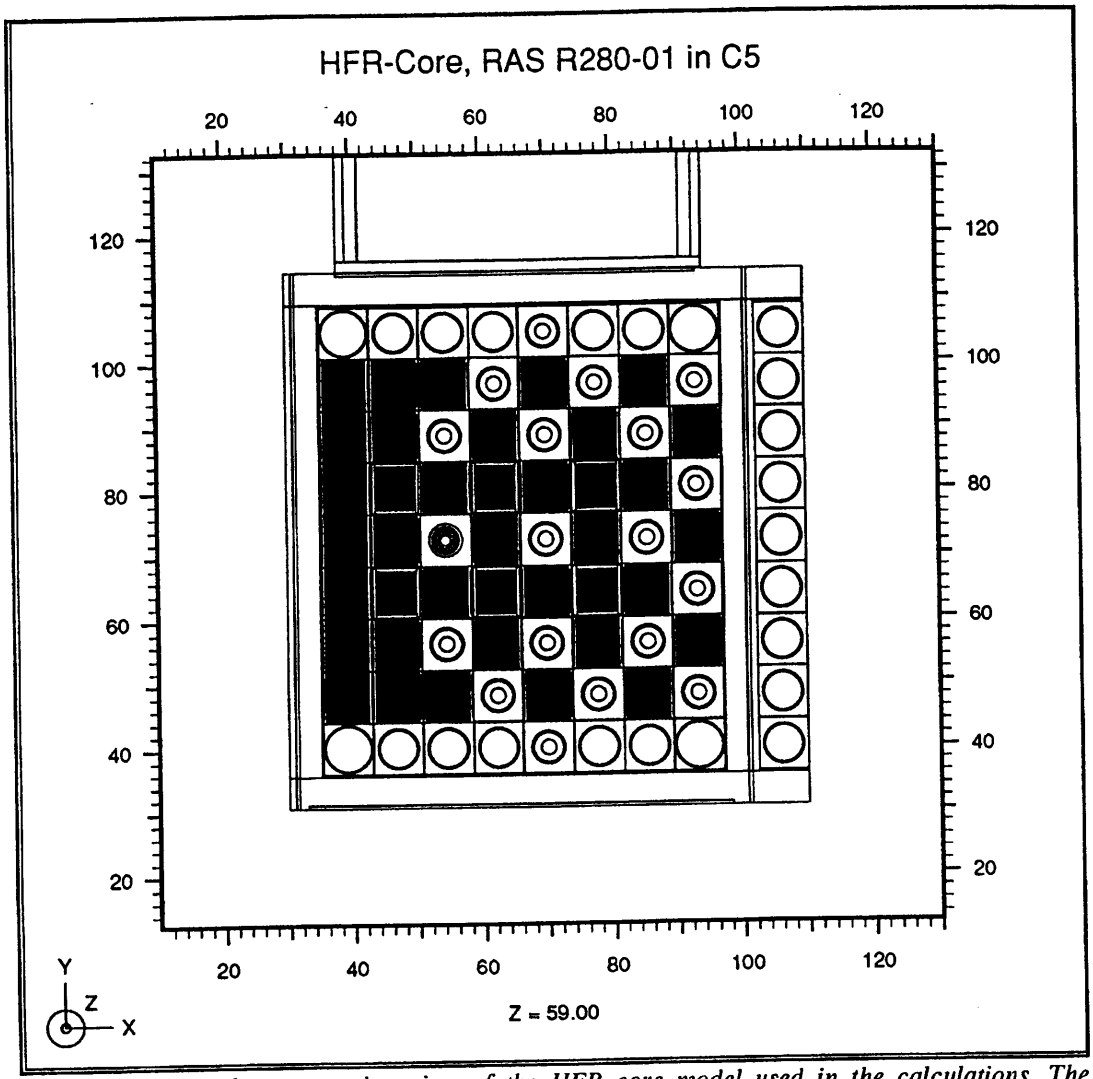

Fig. 6: *Horizontal cross section view of the HFR core model used in the calculations. The experimental facility is loaded at position C5 with (x,y) coordinates (55,73).*

The calculations yield the integrated number of $^{54}Fe(n,p)$ and $^{59}Co(n,\gamma)$ reactions in the detector foils, the ruthenium concentration averaged over each of the two rods, the axially averaged radial distribution and the radially averaged axial distribution in the two rods.

The integrated number of $^{54}Fe(n,p)$ and $^{59}Co(n,\gamma)$ reactions in the detector foils are given in table 3. It is seen that the calculated neutron spectra at the detector positions are quite accurate. The two foils closest to the investigated technetium rod (numbers 6 and 7) give results within 7% for the fast $^{54}Fe(n,p)$ reaction and within 1% for the thermal $^{59}Co(n,\gamma)$ reaction.

Table 3: *Calculated reactions in the ^{54}Fe and ^{59}Co detector foils and the associated C/E ratios.*

Detector foil	$^{54}Fe(n,p)$ (10^{21} cm^{-2})	C/E ratio	$^{59}Co(n,\gamma)$ (10^{21} cm^{-2})	C/E ratio
1	4.84±0.10	1.02±0.02	3.67±0.05	1.03±0.02
2	4.80±0.10	1.01±0.02	3.66±0.05	1.02±0.01
3	4.89±0.10	1.03±0.02	3.63±0.06	0.97±0.02
4	4.94±0.10	1.05±0.02	3.67±0.05	1.01±0.01
5	5.10±0.10	1.08±0.02	3.69±0.06	1.01±0.02
6	5.05±0.10	1.07±0.02	3.57±0.05	1.00±0.01
7	4.86±0.10	1.03±0.02	3.58±0.05	1.01±0.01
8	5.02±0.10	1.05±0.02	3.63±0.05	1.01±0.01
9	5.06±0.10	1.07±0.02	3.57±0.05	0.99±0.01
Average		1.05±0.02		1.01±0.02

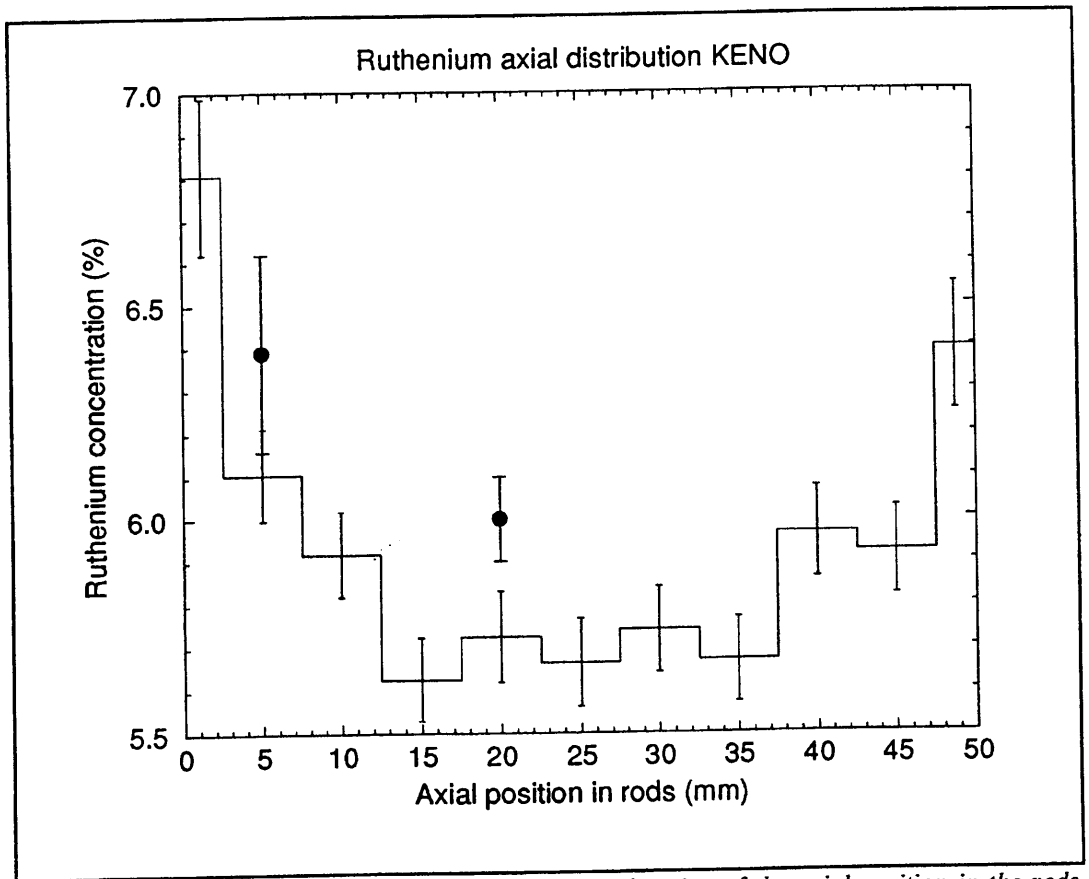

Fig. 7: *The calculated ruthenium concentration as a function of the axial position in the rods. The dots indicate the measurement values at D1 and D2.*

The axial distribution of the ruthenium concentration in the two rods calculated by the Monte Carlo code KENO is shown in figure 7 as a function of the axial position in the rods. Also the two measurement values at D1 and D2 are shown. The lower rod (0<z<25 mm) has been examined by ECN. The vertical bars at each interval denote one standard deviation due to the Monte Carlo process. Clearly the ruthenium concentration shows an axial gradient, but the volume averaged ruthenium concentration of the lower rod (5.92±0.05%) does not differ significantly from that of the upper rod (5.87±0.05%). These calculations support the measured axial gradient as shown in figure 5. The calculated ruthenium concentrations at intersections D1 and D2 have values of 6.10±0.11% and 5.72±0.10%, respectively, which are in reasonable agreement with the measured values given in table 2 (6.39±0.23% at D1 and 5.98% at D2).

The radial distribution of the ruthenium concentration averaged over the two rods in axial direction is shown in figure 8. Clearly, the calculated distribution is not in agreement with the EPMA measurements. Most probably, this is due to the resonance shielding method used in the resolved energy range. By use of the Nordheim method, pin-averaged goup cross sections are calculated which conserve the total neutron absorption. However, due to resonance absorption, the group cross sections change as a function of the distance to the moderator-rod interface.

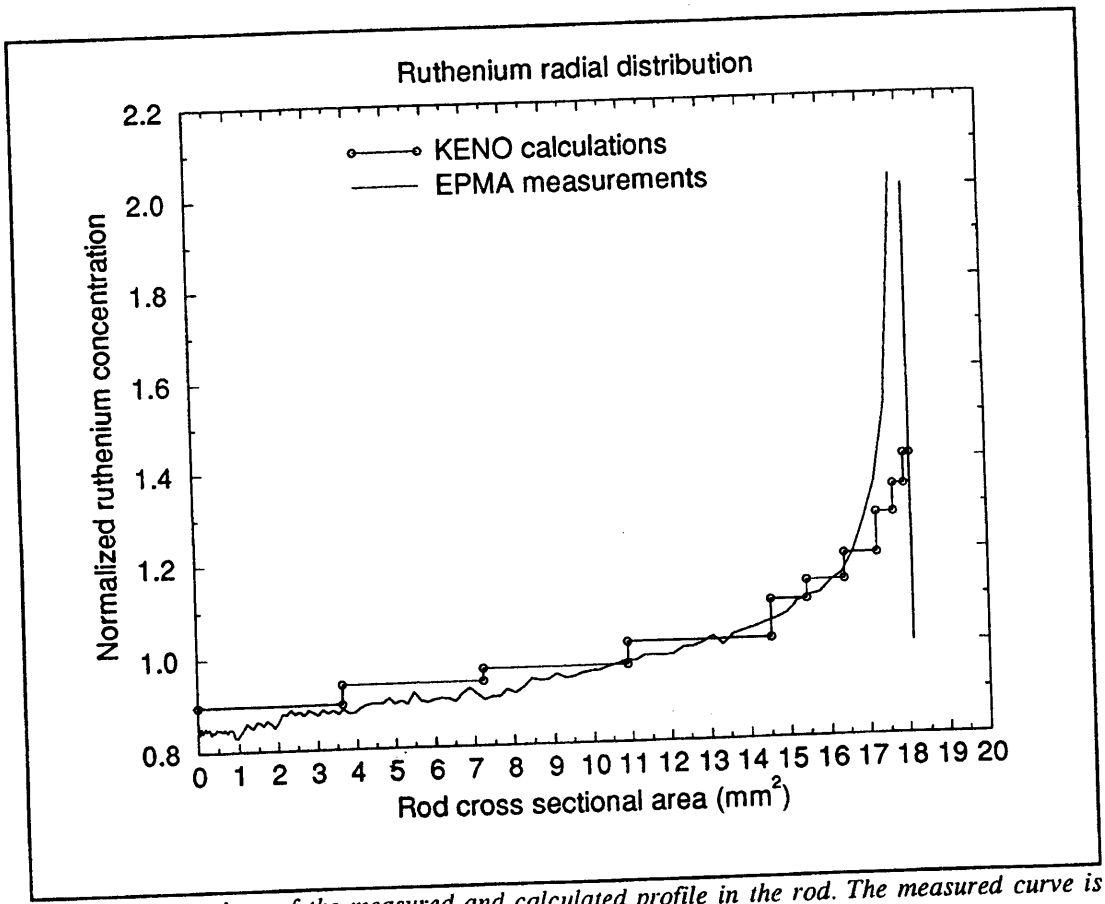

Fig. 8: *Comparison of the measured and calculated profile in the rod. The measured curve is the average of the four curves shown in figures 3 and 4.*

To demonstrate the inadequacy of the Nordheim resonance shielding method for these purposes, a simple one-dimensional model of the experiment has been defined and the radial distribution of the ruthenium concentration has been calculated by both the KENO and the MCNP-4A [7] Monte Carlo codes. The latter code uses a point-wise cross-section library also based on the JEF2.2 nuclear data file. The results are shown in figure 9, where the radial distribution of the ruthenium concentrations normalized to the same value are shown together with the results of the EPMA measurements. Clearly, the MCNP results are in much better agreement with the measurements than the KENO results, due to the point-wise sampling of the cross sections. It is emphasized, however, that the model used in this benchmark is only a simple one-dimensional mockup of the actual experiment. Therefore, the differences between the KENO and MCNP results are meaningful, while the (small) differences between the calculations and the EPMA measurements may be due to the simplified geometry.

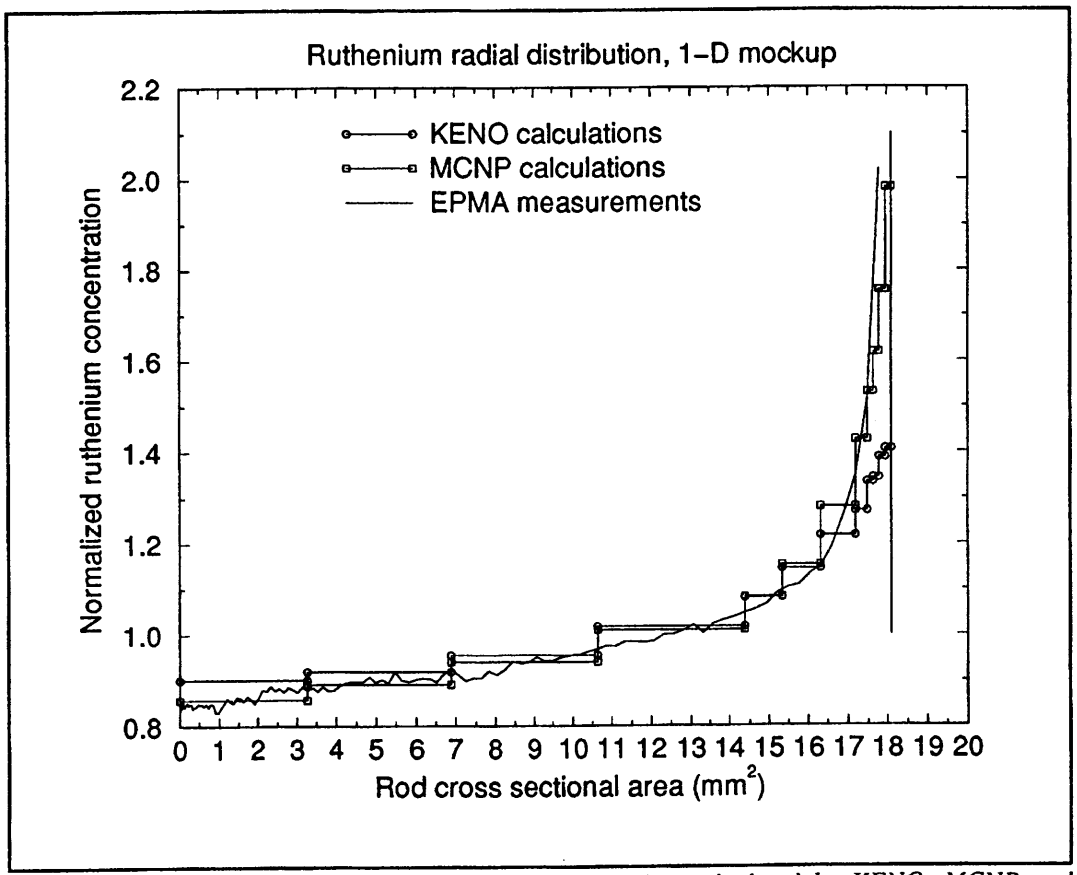

Fig. 9: *The radial profile of the ruthenium concentration calculated by KENO, MCNP and measured by EPMA.*

Conclusions

Six metallic ^{99}Tc rods have been irradiated in the Petten thermal High Flux Reactor with a total neutron fluence of 2 10^{22} cm^{-2}. About 6% of the ^{99}Tc has been transmuted to the stable ^{100}Ru.

The absolute ruthenium concentrations in the rod have been measured by Isotope Dilution Mass Spectrometry, and the radial and axial profiles of the ruthenium concentration have been measured by Electron Probe Micro Analysis (EPMA). The measured ruthenium concentration in the rod ranges from 6.4% at 5 mm from the bottom of the rod (intersection D1) to 6.0% at 5 mm from the top (intersection D2).

Calculations have been performed by the group-wise Monte Carlo code KENO in a detailed three-dimensional model of the HFR core. The calculated ruthenium concentrations of 6.1% at intersection D1 and 5.7% at D2 are in reasonable agreement with the measurements. This shows the validity of the HFR core model and of the cross sections used.

The group-wise Monte Carlo code KENO in combination with the cross-section generation code NITAWL-II (Nordheim resonance shielding method) cannot be used to calculate accurately the radial distribution of the ruthenium concentration in the rods. A Monte Carlo code using point-wise cross sections like MCNP appears to give much better results.

Further work on the transmutation of ^{99}Tc consists of the re-irradiation of two ^{99}Tc rods in the Petten HFR up to a transmutation level of 20%, and the measurement of the thermal absorption cross section. According to reference 8, the thermal capture cross section of ^{99}Tc is 10 to 15% higher than the value in the JEF2.2 evaluated nuclear data file (about 19 barn).

References

[1] J.F. Babelot *et al.*, "EFTTRA Irradiation Experiments for the Development of Fuels and Targets for the Transmutation", This Conference, September 1996.

[2] R.J.M. Konings *et al.*, "Transmutation of Technetium and Iodine - Irradiation Tests in the Frame of the EFTTRA Cooperation", submitted to Nuclear Technology, 1996.

[3] L.M. Petrie and N.F. Landers, "KENO-Va: An Improved Monte Carlo Criticality Program with Supergrouping", ORNL, Tennessee, USA, August 1990.

[4] R.C.L. van der Stad *et al.*, "EIJ2-XMAS: Contents of the JEF2.2 based Neutron Cross-Section Library in the XMAS Group Structure", Netherlands Energy Research Foundation (ECN), Petten, The Netherlands, Report ECN-CX-95-087 (confidential), February 1996.

[5] N.M. Greene *et al.*, "NITAWL-II, SCALE Module for Performing Resonance Shielding and Working Library Production, ORNL, Tennessee, USA, June 1989.

[6] N.M. Greene, "BONAMI-S, Resonance Self-Shielding by the Bondarenko Method", ORNL, Tennessee, USA, August 1981.

[7] J.F. Briesmeister, ed., "MCNP-4A: A General Monte Carlo Code for Neutron and Photon Transport", LANL, Los Alamos, USA, LA-7396-M, Rev. 2, 1986.

[8] H. Harada *et al.*, "Measurement of Thermal Neutron Cross Section and Resonance Integral of the Reaction $^{99}Tc(n,\gamma)^{100}Tc$", J. of Nuclear Science and Technology, vol.32, no.5, pp 395-403 (1995).

STUDIES ON ACCELERATOR-DRIVEN TRANSMUTATION AT JAERI

T. Takizuka, T. Nishida, T. Sasa, H. Takada, and M. Mizumoto

Japan Atomic Energy Research Institute
Tokai-mura, Naka-gun, Ibaraki-ken 319-11 Japan

Abstract

Research and development on intense proton accelerator-driven transmutation of long-lived radioactive nuclides are being carried out at the Japan Atomic Energy Research Institute (JAERI) under the Japanese long-term program for research and development on nuclide partitioning and transmutation technology, called the OMEGA Program. In the conceptual design study of transmutation system, two options of solid system and molten-salt system have been pursued as dedicated transmutation systems with hard neutron spectrum and high neutron flux. Spallation integral experiments are being made on a lead assembly with 500 MeV proton beam to validate and improve the cascade code NMTC/JAERI. Front-end components for the prototype intense proton accelerator such as ion source, RFQ, DTL, and RF source were developed and tested successfully. JAERI is proposing the development of an intense proton linear accelerator of 1.5 GeV class with a maximum beam power of around 10 MW for tests in accelerator-driven transmutation technology and various experiments in basic sciences. The project of the accelerator-based research complex is expected to be launched in 1997 with conceptual designs of the accelerator and research facilities.

1. Introduction

Under the framework of the Japanese long-term research and development program on nuclide partitioning and transmutation (P-T) technology, called the OMEGA Program, the Japan Atomic Energy Research Institute (JAERI) is carrying out R&Ds on P-T [1,2]. The OMEGA Program is aiming at establishing P-T technologies to provide an attractive option for high-level waste (HLW) management in the future. The technologies under study include an advanced partitioning to separate HLW into four element groups [3], transmutation with actinide burner reactor [4], and transmutation with accelerator-driven system. The proposed transmuters are dedicated systems specifically designed for nuclear waste transmutation purpose. With dedicated transmuters, the fuel cycle for P-T can be separated completely from the conventional commercial fuel cycle for power reactors, forming a double strata structure of nuclear fuel cycle [5].

The project on accelerator-driven transmutation technology at JAERI includes the conceptual design study of transmutation plants, the development of spallation simulation code system [6], the spallation integral experiment [7], and the development of a high-intensity proton linear accelerator [8].

In the conceptual design study of accelerator-based transmutation plant, two types of dedicated system concepts are being investigated; solid system and molten-salt system. The design of the solid system is based on the current technology and design practice for sodium-cooled fast breeder reactors. Another option is the molten-salt system with flowing actinide chloride that plays three principal roles of as fuel, target material, and coolant. Its main advantage is the capability of continuous on-line processing of actinides and reaction products.

JAERI is proposing the development of an intense proton linear accelerator for tests in accelerator-driven transmutation technology together with various experiments in basic sciences. The project is called the Neutron Science Project. The proposed accelerator will be of 1.5 GeV class with a final beam power of around 10 MW. It will share the beam among research facilities, which altogether form an accelerator-based research complex.

This paper describes the conceptual designs of accelerator-driven solid system and molten-salt system for nuclear waste transmutation. Outline of the program plan of tests in accelerator-driven transmutation is presented.

2. Accelerator-Driven Transmutation Syetem

JAERI is aiming to develop technologies of an advanced partitioning process of transuranic elements (TRUs) and long-lived fission products from HLW and dedicated systems for their subsequent transmutation. The dedicated transmutation system is specially designed to burn minor actinides (MAs) efficiently in a very hard neutron energy spectrum and high neutron flux.

In this context, JAERI has been pursuing feasible concepts of accelerator-driven system as dedicated transmuters to be introduced in the second stratum (P-T fuel cycle) of the double stratum fuel cycle. The concept of the double stratum fuel cycle is schematically depicted in Fig. 1.

In the conceptual design study of accelerator-driven transmutation plant, two types of system concepts are being investigated. One is the solid system consisting of tungsten target and solid fuel core cooled by liquid sodium. Mononitride fuel is selected mainly on the basis of its good thermal performance and adaptability of dry reprocessing. The design of the solid system is based on the current technology and design practice for sodium-cooled fast breeder reactors.

Another advanced option is the molten-salt system with flowing chloride fuel. The molten-salt fuel also serves as target material and as coolant. One of the main advantages of fluid fuel is the capability of continuous on-line processing of actinides and reaction products. Chloride salt is selected mainly on the basis of actinide solubility.

2.1 Solid System

The design of the solid target/core system is based on the state of the art of technology for a sodium-cooled fast breeder reactor. An accelerator injects proton beam through a beam window into the solid tungsten target located at the center of the target/core. Surrounding the target is the subcritical core loaded with actinide nitride fuel. Spallation neutrons emitted from the target induce further fission in the actinide core region.

The target consists of multiple layers of tungsten disk with through holes for coolant passage. The target is designed to maximize the number of emitted neutrons and to flatten the shape of axial distribution of

neutron flux. The coolant holes are arranged to stagger from layer to layer to avoid the possibility of direct penetration of high energy particles through the target.

The target/core is surrounded by reflectors made of stainless steel. The target and fuel subassemblies are cooled by forced upward flow of primary sodium. The whole target/core including reflectors is contained within a target/core vessel made of steel as shown in Fig. 2. The target/core is of loop type configuration, having two sodium primary loops. A vertical duct for beam path is inserted into the target/core vessel down to just above the target region. The bottom end of the duct is the hemispherical beam window made of oxide dispersion strengthened (ODS) steel. The beam window is cooled by impinging coolant flow from the target exit.

Mononitride of minor actinides is used as fuel in the design of the solid system. Nitride fuel has advantages of a high thermal conductivity around 15 W/m/K and a high melting point around 3100 K. This excellent thermal performance permits a high linear rating and high power density, leading to a high transmutation rate. It also results in a low fission gas release.

High atom density of actinides is beneficial to achieve a hard neutron energy spectrum. This is also preferable to realize a dense fuel cycle for the second fuel cycle stratum, where actinides are maintained in a high concentration throughout the whole cycle [9]. The mutual miscibility of actinide mononitrides also leads to the fuel design of high concentration of actinide elements and simplifies the process of fuel fabrication. For reprocessing, an innovative fuel cycle combined with molten-salt electrorefining will be available in the case of nitride as well as metallic fuel.

With a 1.0 GeV-22 mA incident proton beam, the target/core having an effective neutron multiplication factor of 0.927 produces 360-MW thermal power. The net MA transmutation rate is approximately 110 kg per year, or 9.7 %/y, at a load factor of 80%.

Heat transport and power conversion systems in the plant design are similar to those for a sodium-cooled fast breeder reactor plant. The heat generated in the target/core is transported through the primary and the secondary sodium loops to the power conversion system. In the energy conversion system, thermal energy is converted into electricity through conventional steam turbine. A part of electric power is supplied to its own accelerator.

Major parameters of the nitride fuel solid system are summarized in Table 1. Further study is needed to detail and optimize the system design, taking full advantage of the excellent thermal performance of nitride fuel.

2.2 Molten-Salt System

A conceptual design study is being performed on a molten-salt target/core system as an advanced option for an accelerator-based transmutation system. Figure 3 schematically shows the proposed molten-salt system concept. Chloride salt with a composition of 64NaCl-5PuCl3-31MACl3 is chosen as the fuel for its sufficiently high actinide solubility. The molten-salt fuel serves also as target material and as coolant. This eliminates the physical and functional separation of target and core, and thus significantly simplifies the target/core configuration.

One of the attractive features of the molten-salt fuel is the possibility of continuous fuel feed and on-line processing of reaction product removal.

The target/core is designed for 800-MW thermal power. Proton beam at 1.5 GeV is injected vertically into the central target/core region through the beam window. The target/core region is surrounded by an internal reflector. Intermediate heat exchangers and salt pumps are installed in the annular region around the internal reflector to reduce radiation damages. The intermediate heat exchangers are of compact type with plate-and-fin configuration, where heat in the primary molten salt is transferred to the secondary fluid of molten fluoride salt.

In the fluid fuel system, the heat removal problem usually appears in the intermediate heat exchangers than in the core itself. External shell-and-tube type heat exchangers of conventional design would require a large volume, leading to an unacceptably high actinide inventory and low transmutation rate for a dedicated transmutation system. In the present design, highly efficient compact type heat exchangers are incorporated within a reactor vessel. This in-vessel heat exchanger arrangement minimizes the total volume of the primary system and thus the total actinide inventory.

Another leading candidate fuel for a fast spectrum molten-salt system is PbCl2-AnCl3 (An: actinide). A preliminary nuclear calculation was made for the lead-based molten-salt system with the same geometry and dimensions as the sodium-based molten-salt system. The energy of incident proton is 1.5 GeV. Table 2 lists the calculated results in comparison with the sodium-based salt system.

A comparison is also made for two candidate molten salts from the point of thermal-hydraulics design view.

Primary flow cross section area S in a heat exchanger can be estimated from the Blasius equation f = 0.3164 Re-0.25 for friction and the Dittus-Boelter equation Nu = 0.023 Re0.8 Pr0.4 for heat transfer, where f = friction factor, Nu = Nusselt number, Re = Reynolds number, Pr = Prandtl number. In case when the maximum fluid velocity is a limiting factor in the design, S is expressed as

$$S = c\,(d\,Q/\lambda)\,(1/\Delta\theta)\,Re^{-1}\,Pr^{-1},$$

where d = hydraulic diameter of the flow channel, Q = thermal power exchanged, λ = thermal conductivity $\Delta\theta$ = temperature drop through heat exchanger. It is noted that S is independent on the temperature difference between primary and secondary coolants. Assumptions were made that the maximum fluid velocity is limited by the pressure drop and the dynamic pressure in the primary system and the viscosity, thermal conductivity, and thermal capacity of the fluid are constant. Under these assumptions, S becomes proportional to the square root of the fluid density ρ. For other primary flow cross sections, the same relation holds if the pressure drop and dynamic pressure are to be unchanged. This results in the relation that the total volume of the primary system varies as $\rho^{1/2}$.

Table 3 compares system parameters of the sodium-based molten-salt system and those of the corresponding lead-based molten-salt system. The total inventory of the lead-based salt in the system is about 65% larger due to its higher fluid density than that of sodium-based salt, but the actinide inventory is about 25% smaller. The comparison is preliminary since reliable data of thermodynamic and transport properties are lacking for lead-based salt.

3. Spallation Integral Experiment

In the design study of accelerator-based transmutation system, a nulceon meson transport code, NMTC/JAERI is used to simulate nuclear reactions and the particle transport in the energy range above 15 MeV. To estimate and validate the accuracy of the code system, a spallation integral experiment using a large scale lead assembly is in progress. The lead assembly is bombarded with 500 MeV protons at the booster synchrotron facility of the National Laboratory for High Energy Physics (KEK).

The lead assembly was 60 cm in diameter and 100 cm in length. The protons were injected through the beam entrance hole into the target of 16 cm in diameter and 30 cm in length installed in the assembly. The target is made of lead or tungsten alloy. High purity metal activation samples of Al, Fe, Ni, Cu and Au were inserted into irradiation holes drilled parallel to the beam axis in the assembly at various radial distances. The gamma-ray spectrometry was used to obtain yields of the nuclides produced in the samples.

Neutron energy spectrum from thick lead target and nuclide yield distributions of various threshold reactions in a lead assembly were measured in the experiment. In general, the calculation with the codes NMTC/JAERI and MCNP4.2 was agreed fairly well with the experimental results.

There are however some discrepancies in both the nuclide production cross section and the neutron energy spectrum, requiring further improvements in the calculation model. Comparison of the yield of proton induced spallation products is planned in the next step in the integral spallation experiment to validate the accuracy of the NMTC/JAERI prediction.

4. Intense Proton Accelerator and Transmutation Test Facility

JAERI is proposing the development of an intense proton accelerator for tests in accelerator-driven transmutation technology together with various experiments in basic sciences. The plan called the Neutron Science Project is aiming at the scientific and technological innovation for the 21st century using neutrons. The study on accelerator-driven transmutation and the development of an intense proton accelerator are under way as the important part of the Project. The proposed accelerator will be of 1.5 GeV class with a beam power around 10 MW and employ superconducting linac in the high-energy portion. It will share the beam among research facilities, comprising an accelerator-based multi-purpose research complex.

To develop intense accelerator technology, R&D work has been carried out for the accelerator components for the front-end part; ion source, radiofrequency quadrupole (RFQ), a drift tube linac (DTL), and RF source. Prototype components of the ion source, RFQ, and RF source have been developed and tested successfully. The design study for an intense proton accelerator is also underway and efforts are focused on a superconducting

accelerating cavity as a main option for the high-energy portion above 100 MeV. The superconducting linac has attractive features for a high-intensity accelerator such as shorter length acceleration, large bore radius resulting in low beam losses and possible cost reduction in the construction and operation. A test stand equipped with cryogenics system, vacuum system, RF system and cavity processing and cleaning is being prepared to test the physics issues and fabrication process.

The preconceptual study for the transmutation experimental facility started in the late 1995. The experimental program is to be proceeded in two steps. The first step will be the feasibility study of the hybrid system concept with a spallation target and a uranium subcritical system at a low power level with a pulsed beam. The experiments will demonstrate the stable operation of a hybrid system and MA burnup with use of MA foils or pellets. It will provide and verify the database for the development and design of a test reactor facility in the second step.

In the second phase, a test reactor facility will be constructed to perform tests of integrated target/core system at a moderate thermal power level of 10-30MW with a CW beam. Transmutation capability of the hybrid system will be tested using MA target pins. These system level tests will demonstrate the technical viability of the accelerator-based transmutation system. Technical feasibility of spallation target and beam window will be also tested at a high beam power in the second step experiments. These experiments are expected to open up possibility for the development of a future nuclear option of accelerator-driven system for not only waste transmutation but also energy production and fuel breeding.

The JAERI Neutron Science Project of the accelerator-based research complex is planned to start in 1997 with conceptual design of the intense proton accelerator, transmutation test facility, and other research facilities. Construction will be started around 1999. Operation with 1.5-MW beam power is expected to begin as early as 2003, and upgrading up to the full beam power around 10 MW will be completed in 2006.

5. Summary

The conceptual designs of accelerator-driven solid system and molten-salt system for nuclear waste transmutation were presented in this paper together with brief outline of the program plan of tests in accelerator-driven transmutation technology.

JAERI accelerator-driven transmutation project is being proceeded under the Japanese long-term R&D program on P-T technology, called OMEGA. In the conceptual design study, both solid system and molten-salt system are being pursued as dedicated transmuters to be introduced in the second stratum of the proposed double stratum fuel cycle system.

In either system, an MA-loaded subcritical core is driven by a high-intensity proton accelerator and makes use of hard neutron energy spectrum to transmute MAs efficiently by fission. The design of the solid system is based on the status of liquid-metal fast reactor technology, whereas the design of the molten-salt system relies on the next generation technology.

The solid system employs actinide mononitride fuel that has several favorable features as fuel for dedicated transmutation systems in the proposed double stratum fuel cycle. Its main advantages are excellent thermal performance and high atom density of actinides. It is expected that further improvement in the transmutation performance can be achieved by taking full advantage of the excellent thermal performance of nitride fuel.

The molten-salt system employs flowing chloride salt fuel which also acts at the same time both as target material and as coolant. The fuel salt selected for the reference design is NaCl-$AnCl_3$. Another leading candidate salt is $PbCl_2$-$AnCl_3$. A preliminary comparative nuclear and thermal-hydraulics design study was made for these two compositions of fuel salts. Results obtained seems to be not conclusive mainly due to the lack of reliable property data for $PbCl_2$-$AnCl_3$.

JAERI is proposing the development of an intense proton linear accelerator with a beam power of around 10 MW for tests in accelerator-driven transmutation technology together with various experiments in basic sciences. The preconceptual study for the transmutation test facility was initiated recently. The project is planned to start in 1997 with conceptual design of the accelerator and research facilities. Operation with 1.5-MW beam power is expected to begin as early as 2003, followed by gradual upgrading to the full beam power around 10 MW.

References

[1] Mukaiyama,T. et al.: "Partitioning and Transmutation Program "OMEGA" at JAERI", Proc. 4th OECD/NEA Int. Information Exchange Mtg. on P-T, Mito (1996).

[2] Saito, S.: "Research and Development Program on Accelerator-driven Transmutation at JAERI", Proc. 2nd Int. Conf. on Accelerator-Driven Transmutation Technologies and Applications, Kalmar (1996).

[3] Kubota, M. et al.: "Development of Partitioning Process in JAERI", Proc. 3rd OECD/NEA Int. Information Exchange Mtg. on P-T, Cadarache (1994).

[4] Mukaiyama, T. et al.: "Minor Actinide Burner Reactor and Influence of Transmutation on Fuel Cycle Facilities", IAEA-TECDOC-783, (1993).

[5] Mukaiyama, T. et al.: "Importance of the Double Strata Fuel Cycle for Minor Actinide Transmutation", Proc. 3rd OECD/NEA Int. Information Exchange Mtg. on P-T, Cadarache (1994).

[6] Nishida,T. et al.: "Development of the Code System ACCEL for Accelerator-Based Transmutation Research", Proc. 2nd Int. Int. Conf. on Accelerator-Driven Transmutation Technologies and Applications, Kalmar (1996).

[7] Takada, H. et al.: "Production of Radioactive Nuclides in a Lead Assembly with 500 MeV Protons", Proc. Specialists' Mtg. on Accelerator-Based Transmutation, PSI (1992).

[8] Mizumoto, M.: "Development of High Intensity Proton Accelerator", Proc. 2nd Int. Conf. on Accelerator-Driven Transmutation Technologies and Applications, Kalmar, (1996).

[9] Suzuki, Y. et al.: "Studies on Nitride Fuel for TRU Burning", Proc. 3rd OECD/NEA Int. Information Exchange Mtg. on P-T, Cadarache (1994).

Table 1 Major Parameters of Nitride Fuel Solid System

Fuel	Mononitride (90MA-10Pu)N MA: Np, Am, Cm
Target	Tungsten Multi-Layer Disk Type
Actinide Core Height	800 mm
Target/Core Volume	0.06/0.35 m^3
Actinide Inventory	1150 kg
Neutron Multiplication Factor	0.927
Proton Beam, Energy - Current	1.0 GeV - 22 mA
Average Neutron Flux	5.2×10^{15} $n/cm^2/s$
Power Density Average/Maximum	1020/1600 MW/m^3
Thermal Power	360 MW
Burnup	110 kg/y (9.7 %/y)
Coolant Temperature Inlet/Outlet	663/793K
Clad Temperature, Maximum	988 K
Fuel Temperature, Peak	1440 K

Table 2 Neutronics of Na-based Salt and Pb-based Salt Systems

	$64NaCl-36AnCl_3$	$70PbCl_2-30AnCl_3$
Neutron Multiplication Factor	0.93	0.88
Spallation Neutron Yield (n/p)	37	40
Average Neutron Energy * (keV)	800	768
Power Density ($keV/cm^3/p$)		
Average*	27	16
Peak	66	54
Peaking Factor	2.5	3.5

* averaged over target/core region, excluding IHX region.

Table 3 Property and System Parameters for Na-based Salt and Pb-based Salt

	$64NaCl-36AnCl_3$	$70PbCl_2-30AnCl_3$
Fluid Density (kg/m^3 at 923K)	3800	5300
Melting Point (K)	~726	~783
Primary System Volume (m^3)	2.7	3.2
Molten-Salt Inventory (kg)	10,000	17,000
Actinide Inventory (kg)	5,400	4,100

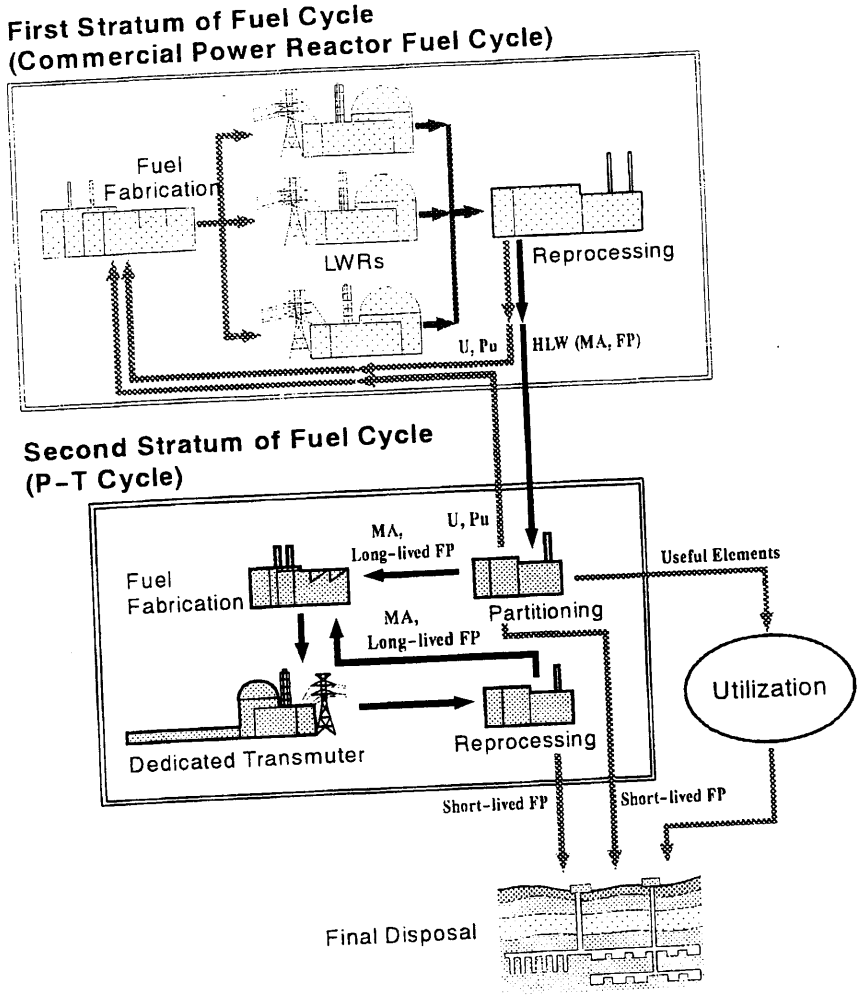

Fig. 1 Double-stratum fuel cycle

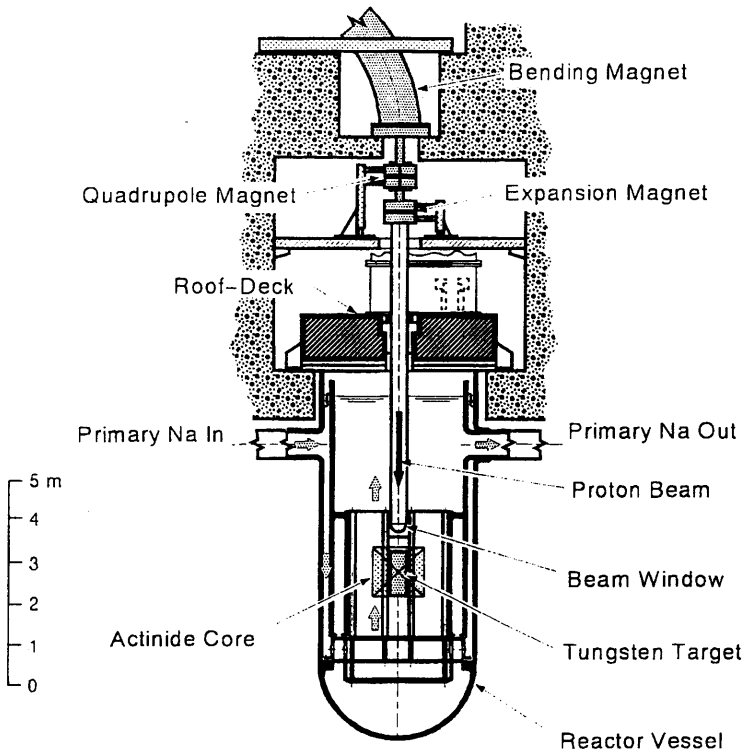

Fig. 2 Accelerator-driven nitride fuel solid target/core system

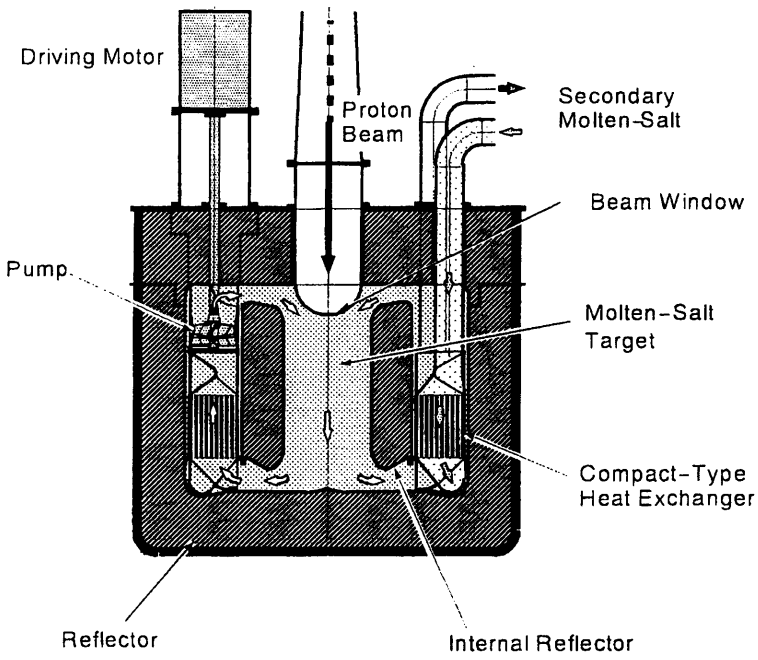

Fig. 3 Conceptual drawing of molten-salt target/core system

A Study on the Transmutation Capability of Accelerator Driven System

Won Seok Park, Hee Sung Shin, Tae Yong Song
Korea Atomic Energy Research Institute

A preliminary investigation was performed to evaluate the capability of accelerator driven thermal neutron system for the transmutation of minor actinides and fission products. Although the accelerator driven thermal neutron system was introduced long before by LANL, there has not been that much of research on minor actinide and fission product burning. LANL has focused its research mainly on the plutonium destruction.
For the analysis, 1GeV, 20mA proton linac was employed and the LAHET code developed by LANL was adopted for the simulation. The systems are molten salt fluoride with graphite moderator and in order to keep the system subcriticality 0.95, the ratio of plutonium to MA was adjusted. For the depletion calculation, ORIGEN2 code was used and systemwise one group cross section was generated by HMCNP.
The system was believed to have the neutronic characteristics something between LWR and FBR. The system was found to have about 14 %/yr transmutation rate for MA with a capacity factor 0.8. However it showed negligible capability for FP.

I. Introduction

Korea Atomic Energy Research Institute (KAERI) has performed a transmutation research since the middle of 1992. It had finished its first stage research in July of 1996 and obtained the tentative conclusion on its future transmutation research direction.

KAERI tried to estimate which option would be the optimal transmutation technology among LWR, FBR, accelerator-driven subcritical reactor concepts. The estimation works were done by evaluating the transmutation capability, the technical feasibility, the resistance to NPT(the possibility of commercialization), the safety, the economical advantages of each concept. A spent fuel problem is not the problem of one or two countries any more. It is the problem of world because nuclear power has been a worldwide energy source. In order to solve that worldwide problem, the technology to be developed should have something that any country can access and employ. From those points of view, weightings were assigned to the NPT resistance, transmutation capability, safety, technical feasibility, economical benefits in descending order. As results, the optimal concept was determined to be an accelerator driven subcritical reactor.

The detail neutronic analysis for an accelerator driven system will be done throughout the second stage research period from 1996 to 1999. No specific design parameters were determined yet. As a starting point, the thermal neutron system with molten salt fuel was selected. In this paper, some basic results obtained from the preliminary studies on the selected system was presented.

II. System Model Description

A program called KOMAC(KOrea Multipurpose linear ACcelerator) is under planning to build 1.0 GeV, 20mA linear proton accelerator in KAERI. KOMAC will be developed in a way to be applicable to transmutation. The proton beam of 1GeV, 20 mA was assumed for the spallation calculation. Basic concepts for the thermal system were derived from the ATW designed by LANL. Fig. 1 shows the schematic layout of the subcritical blanket and Table 1 represents the material specifications of the system. Lead target with the diameter 75cm and the height 100 cm was employed to get the neutrons induced by spallation reaction and graphite was adopted for neutron moderation. Because of very low solubility of TRU in molten fluoride, 1.0 mol% of TRU was assumed and the chemical form of fuel was $66LiF\text{-}33BeF_2\text{-}1(TRU)F_4$. The reason using fluoride instead of chloride is to enhance the neutron moderation. The operating temperature was assumed to be 650°C and the physical density of molten salt was at the operating temperature. Because a thermal neutron is the most effective tool for fission product burning, a couple of sites were assigned for fission product incineration in the graphite region.

III. Calculational Methodology

LCS(LAHET code system) developed by LANL was employed to perform the neutronic analysis in the sample model. LAHET and HMCNP are the main codes in LCS.[1] Fig. 2 shows the input-output flow between codes. By adjusting the amount of Pu in total TRU, the subcriticality was kept to be 0.95. LAHET code analyzes the spallation reactions and deals with high energy neutrons(>20MeV).[2] LAHET provides HMCNP with a sort of fixed external neutron sources(energy and location). HMCNP performs the calculation of neutron flux and thermal power in the blanket.[3] HMCNP generated one group, corewise cross sections to be used for the calculation of transmutation capability using ORIGEN2.[5]

IV. Results

By using the kcode function in MCNP code, the nuclide composition of TRU to keep the system subcriticality 0.95 was searched. In that condition, the nuclide composition of Pu and MA was found to be 72:28 and the loading amount of MA was 775 kg.

The isotope composition of lead target was that of natural lead(Pb-204:Pb-206:Pb-207:Pb-208=2:24:22;52). The neutron production rate depends on the isotope composition and the size of the target. The more stable the nuclide is, the less the neutron production rate is. The neutron production rate was 34n/p in the proposed system and Fig. 3 shows the number of neutrons produced by the spallation reaction versus its energy. The figure shows that the most of spallation neutrons have the energy ranging from 2MeV to 10 MeV which is much higher than the fission neutron energy. A considerable amount of heat is generated by spallation reaction. In the proposed model, 1.3MW was deposited in the target.

As it is expected, maximum flux occurs at the target region. The average neutron flux in the target is about 80 ~ 90 times higher than that of blanket while the neutron flux of the reflector is 10 times less than that of blanket. Table 2 gives the neutronic parameters generated. For a given condition, the system produced the thermal power of 967 MW. Fig.4, 5 show the neutron energy spectrum in the blanket, and graphite region, respectively. In order to evaluate the transmutation capability, one group cross sections for 21 actinides and 17 fission product nuclides were produced using the average neutron energy spectrum in the blanket and reflector region, respectively. Table 3, 4 represent the transmutation capability of the system for actinides and fission products, respectively. The proposed system is supposed to transmute MA with the rate of 14%/yr when a capacity factor is assumed to be 0.8. On the other hand, it has negligible capability for fission product burning.

V. Discussion and Conclusion

A preliminary calculation was done to evaluate the neutronic performance of the accelerator driven thermal neutron system. Because the criticality of the system was 0.95, about 5% of neutrons were come from the spallation reaction. Therefore the average source neutron energy is supposed to be somewhat higher than the fission neutron energy. In addition, the moderator was positioned in a way to surround the blanket like a reflector. Such an array can not moderator the high energy neutron efficiently. As results, the neutron energy spectrum of the system was found to be something between LWR and FBR. Epithermal neutron can be suggested to be more effective for the transmutation. It might be true for some nuclides but not for some others. Table 5 shows one group absorption cross sections of some important long lived fission products. This table tells that the proposed system is more efficient for burning I-129 while LWR is for Tc-99. The system was believed to have a considerable capability for MA transmutation. On the other hand, it had negligible for fission products. The main reason for that was due to the difference in the neutron flux. Therefore FP burning sites should be moved to somewhere a high neutron flux can be obtained. As it is known, a thermal neutron has an advantage of higher MA transmutation capability and a disadvantages of producing lots of higher actinides while a fast neutron has a reverse characteristics. Further detail studies should be done to decide which neutron is more efficient for the transmutation. Also some attention has to be paid on the definition of the transmutation when only MA is considered to be transmuted. In other words, it has to be answered whether it is transmutation or not when Np-237 is transformed to Pu by the successive absorption.

References

[1] Richard E. Prael and Henry Lichtenstein, User Guide to LCS : The LAHET Code Systems, LA-UR-89-3014, Los Alamos National Lab. (1989)

[2] R. G. Alsmiller et al., The High Energy Transport Code HETC88 and Comparisons with Experimental Data, Nucl. Inst. and Meth. In Phys. Res., A295, pp337-343.

[3] Judith F. Briesmeister, MCNP-A General Monte Carlo N-Particle Transport Code Version 4A, LA-12625-M.(1993)

[4] Carl A. Beard et al., Parameteric System Studies of the Aqueous-based (slurry) Balnket Concept for Accelerator Transmutation of Waste, Nucl. Tech. Vol. 110 (1995)

[5] A. G. Groff, A User Manual for the ORIGEN2 Computer Code, ORNL/TM-7175, ORNL(1980)

[6] Judith A. Benzdecny et al., Preliminary Analysis of the Induced Structural Radioactivity Inventory of the Base-case Aqueous Accelerator Transmutation of Waste Reactor Concept, Nuclear Technology, Vol 110(1995)

Table 1 Material Specifications for the proposed system

Component	Specifications
Target	• Material : Lead • Density : 11.34 g/cm^3 • Nuclide Composition : Pb-204:206:207:208=2:24:22:52
Fuel	• Chemical Form : Molten Salt (66LiF-33BeF_2-(TRU)F_4) • Density : 2.06 g/cm^3 • TRU Composition : Pu/MA = 72/28
Moderator	• Material : Natural Graphite • Density : 2.25g/cm^3
Target and Blanket Container	• Material : HT-9 • Density : 7.75 g/cm^3 • Composition : Fe: Ni : Cr: Mo: Mn = 67.50:11.25:17.0:2.25:2.0 (at./wt.%)

Table 2 Some Neutronic Parameters

Parameter	Target Region	Blanket Region	Graphite Region
Spallation Neutron	34 n/p	negligible	negligible
Avg. Flux(10^{14}n/cm^2-sec)	656.0	8.2	0.88
Thermal Power	4.8	966.6	0.05

Table 3 Transmutation Rate for MA

(unit : kg , kg/yr)

Nuclide	Loading Amount	After-30-days	Amount[a] (kg/yr)	Rate[b] (%/yr)
^{237}Np	3.419E+02	3.296E+02	-1.476E+02	-43
^{238}Np	0.000E+00	1.231E+00	1.477E+01	-
^{238}Pu	3.062E+01	4.163E+01	1.321E+02	431
^{239}Pu	1.155E+03	1.113E+03	-5.040E+02	-44
^{240}Pu	5.269E+02	5.335E+02	7.920E+01	15
^{241}Pu	1.701E+02	1.715E+02	1.680E+01	10
^{242}Pu	9.945E+01	1.016E+02	2.580E+01	26
^{241}Am	3.710E+02	3.473E+02	-2.844E+02	-77
^{242m}Am	0.000E+00	9.869E+00	1.184E+02	-
^{242}Am	0.000E+00	4.311E-01	5.173E+00	-
^{243}Am	6.119E+01	5.492E+01	-7.524E+01	-123
^{242}Cm	0.000E+00	1.038E+01	1.246E+02	-
^{243}Cm	1.950E-01	2.144E-01	2.328E-01	119
^{244}Cm	1.147E+01	1.959E+01	9.744E+01	850
^{245}Cm	6.290E-01	1.062E+00	5.196E+00	826
U	0.000E+00	3.045E-02	3.654E-01	-
Np	3.419E+02	3.308E+02	-1.332E+02	-39
Pu	1.982E+03	1.961E+03	-2.520E+02	-13
Am	4.321E+02	4.126E+02	-2.340E+02	-54
Cm	1.230E+01	3.125E+01	2.274E+02	1849
MA*	7.863E+02	7.747E+02	-1.398E+02	-18
TRU**	2.768E+03	2.736E+03	-3.918E+02	-14
ACT***	2.768E+03	2.736E+03	-3.914E+02	-14

* Total minor actinide nuclides, ** Total transuranium nuclides, *** Total actinide nuclides.

a) (loading amount - after-30day amount)*365/30.

b) (transmutation amount/loading amount) *100.

Table 4 Transmutation Rate of Fission Products

(unit : kg, kg/yr)

Nuclide	Loading Amount	After-1-year Amount	Amount[a)] (kg/year)	Rate[b)] (%/year)
^{99}Tc	2.60E+02	2.59E+02	-6.00E-01	-0.23
^{100}Ru	0.00E+00	5.64E-01	5.64E-01	-
^{127}I	1.51E+01	1.51E+01	-2.00E-02	-0.13
^{128}Xe	0.00E+00	1.63E-02	1.63E-02	-
^{129}I	4.87E+01	4.86E+01	-6.00E-02	-0.12
^{130}Xe	0.00E+00	6.07E-02	6.07E-02	-
^{133}Cs	3.14E+01	3.13E+01	-9.00E-02	-0.29
^{134}Cs	0.00E+00	7.43E-02	7.43E-02	-
^{134}Ba	0.00E+00	1.32E-02	1.32E-02	-
^{135}Cs	8.36E+00	8.36E+00	-4.00E-03	-0.05
^{136}Ba	0.00E+00	4.49E-03	4.49E-03	-
^{137}Cs	2.65E+01	2.59E+01	-6.00E-01	-2.27
Tc	2.60E+02	2.59E+02	-6.00E-01	-0.23
Ru	0.00E+00	5.65E-01	5.65E-01	-
I	6.38E+01	6.37E+01	-8.00E-02	-0.13
Xe	0.00E+00	7.70E-02	7.70E-02	-
Cs	6.62E+01	6.56E+01	-6.20E-01	-0.94
Ba	0.00E+00	6.22E-01	6.22E-01	-
Total LLFP*	3.90E+02	3.89E+02	-1.30E+00	-0.33
Total FP*	3.90E+02	3.90E+02	-3.62E-02	-0.01

* Total amount of long-lived fission products.
** Total amount of fission products.
a) (loading amount - after-30day amount)*365/30.
b) (transmutation amount/loading amount) *100.

Table 5 Absorption Cross Section Comparison for Major FPs

(unit : barn)

Nuclide	Absorption Cross Section		
	Proposed System	PWR	FBR
^{99}Tc	6.910E+00	9.136E+00	4.767E-01
^{127}I	5.984E+00	4.846E+00	5.450E-01
^{128}Xe	2.547E+00	6.541E-01	1.709E-01
^{129}I	7.140E+00	3.225E+00	3.757E-01
^{130}Xe	1.518E+00	6.260E-01	1.074E-01
^{131}Xe	4.881E+01	3.046E+01	2.130E-01
^{133}Cs	1.296E+01	1.072E+01	4.845E-01
^{134}Cs	3.330E+01	1.675E+01	5.366E-01
^{135}Cs	4.085E+00	2.391E+00	7.307E-02
^{137}Cs	3.843E-02	2.559E-02	1.303E-02

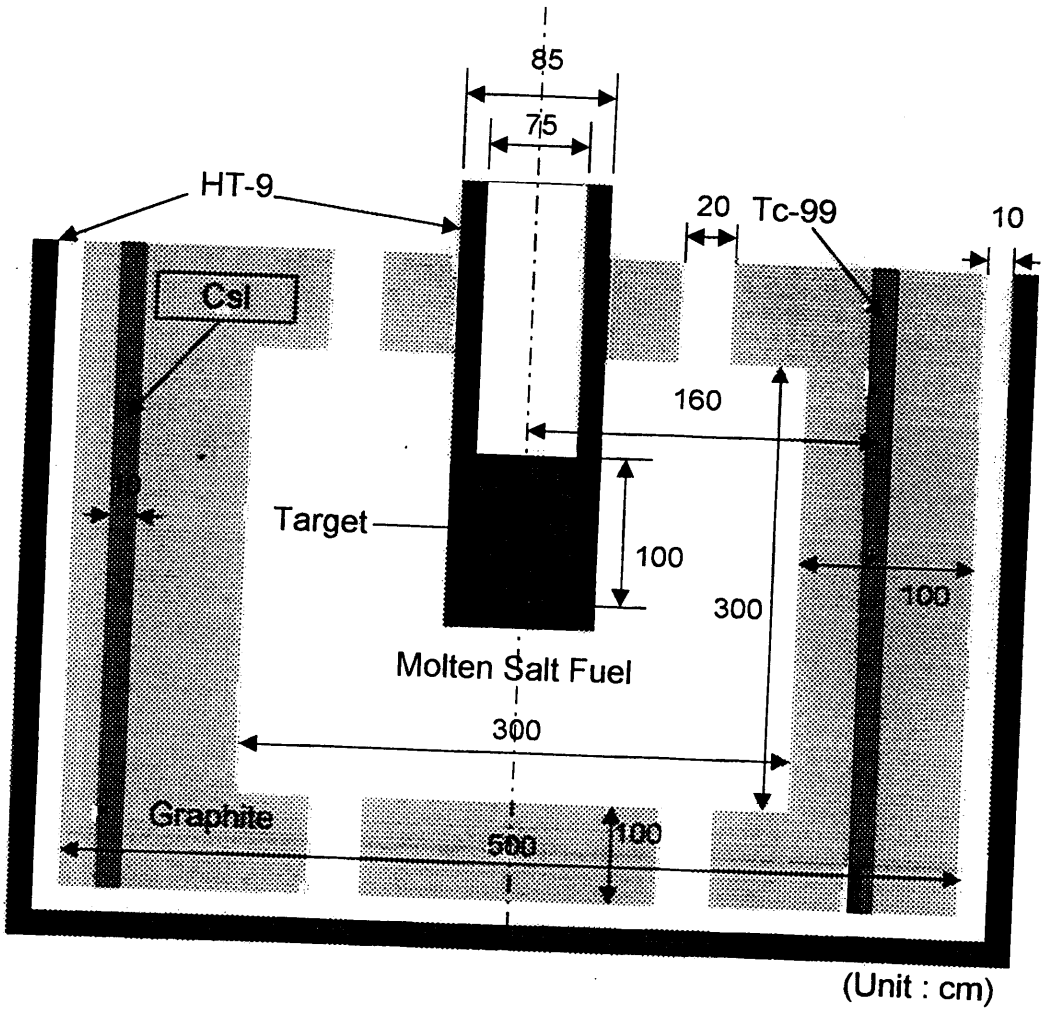

Fig.1 Schematic Layout of the System.

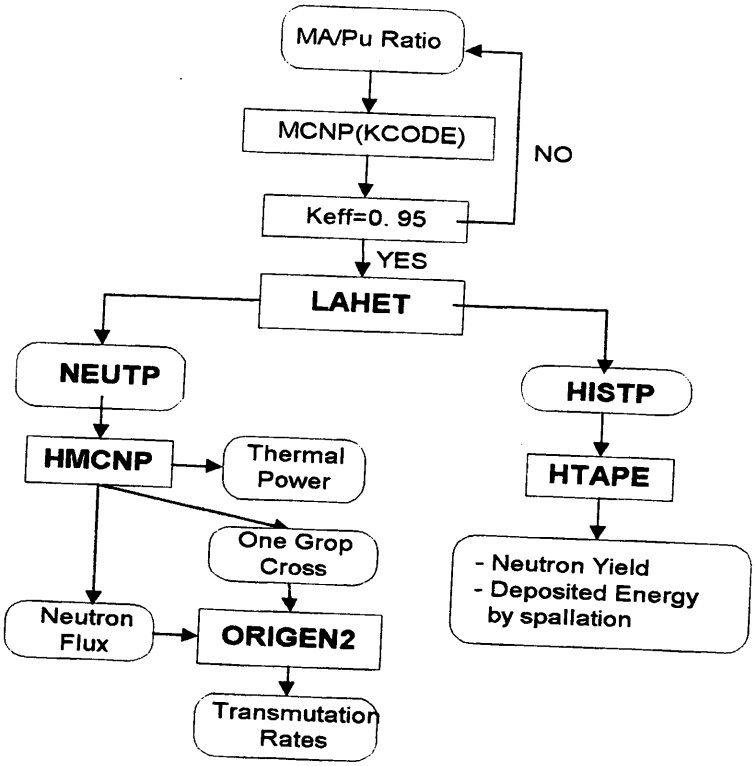

Fig.2 Data Flow between Codes

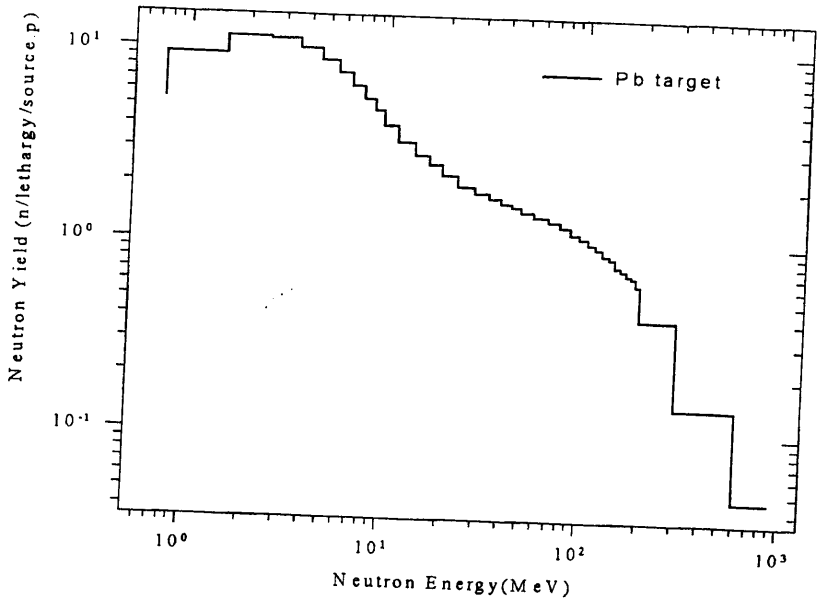

Fig.3 Spallation Neutron Energy Spectrum

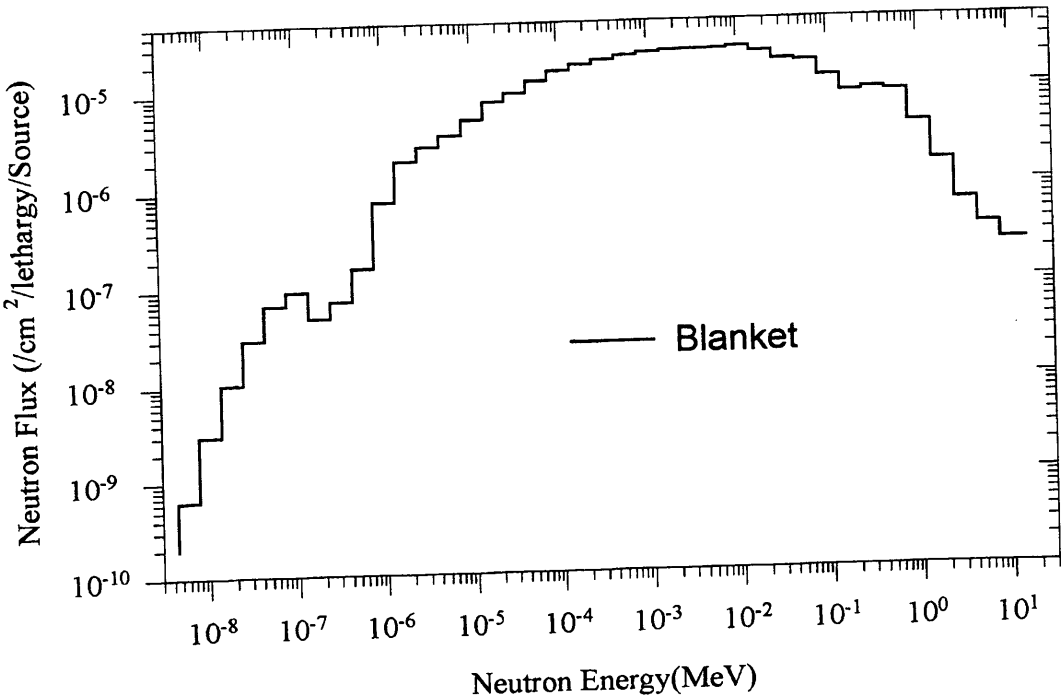

Fig. 4 Neutron Energy Spectrum in Blanket

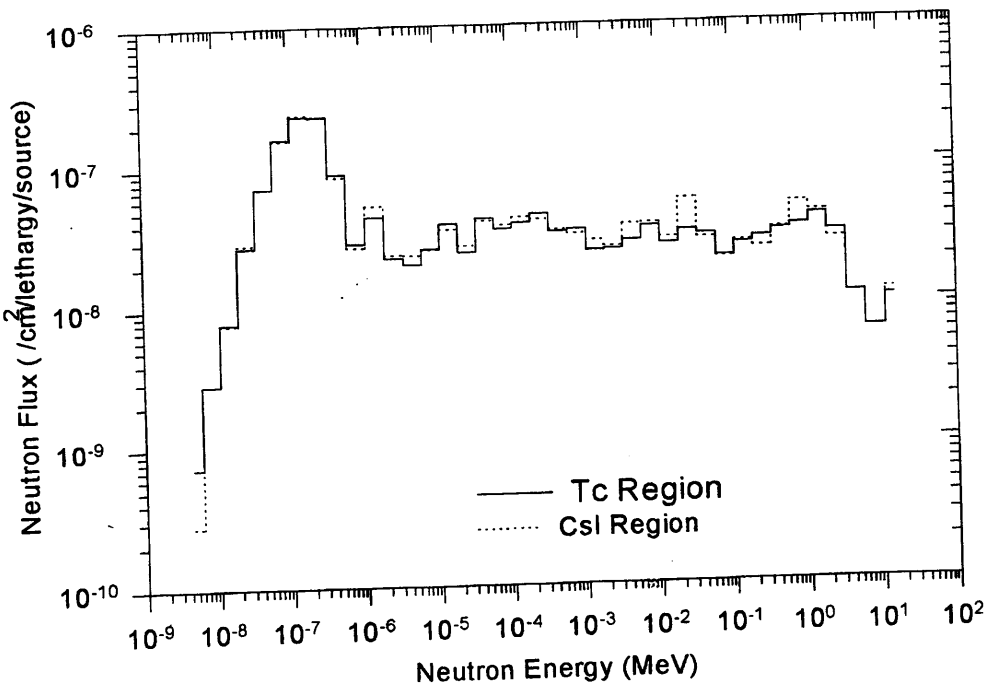

Fig. 5 Neutron Energy Spectrum in FP Burning Region

RESEARCH AND DEVELOPMENT OF NITRIDE FUEL CYCLE FOR TRU BURNING

Yasufumi Suzuki, Toru Ogawa, Toshitaka Osugi, Yasuo Arai, and Takehiko Mukaiyama
Japan Atomic Energy Research Institute
Tokai-mura, Naka-gun, Ibaraki-ken, 311-13 JAPAN

The present status of the research and development of nitride fuel cycle for burning transuranium elements in actinide burner reactors and fast reactors at JAERI is described, especially focusing on the progress in the recent two years. The research and development cover fuel fabrication technology, property measurements such as thermal conductivity, basic irradiation tests at Japan Materials Testing Reactors(JMTR), electrorefining of actinide nitrides in fused salts, and the evaluation of mass balance in the reprocessing process of nitride fuel.

1. Introduction

Actinide nitrides provide advantageous thermal properties such as high thermal conductivity and high melting temperature. By applying the cold fuel concept[1] to fuel design for the transmutation of minor actinides (Np, Am and Cm), it would become possible to realize lower fuel temperature and hence lower fission gas release. Therefore, thinner cladding material might be acceptable and neutron spectrum could be harder. Furthermore, the mutual miscibility of actinide mononitrides might also lead to the fuel design with high concentrations of transuranium elements(TRUs). Considering the characteristics of nitride fuel, the actinide burner reactor(ABR) concept with a nitride fuel cycle has been proposed from Japan Atomic Energy Research Institute(JAERI) [2]. The research and development on nitride fuel cycle carried out at JAERI include fabrication technologies, property measurements, irradiation tests, and electrorefining of TRU-bearing nitride fuel. In addition to the above experimental studies, the mass balance in the pyroprocess has been evaluated. In the present report the progress of the studies on the nitride fuel cycle after the previous meeting[3] is mainly described.

2. Fuel Fabrication

2.1 Fabrication of nitride fuel particles by sol-gel method

The fabrication technology of nitride particle fuel by a sol-gel method has been investigated[3]. Minor actinides separated from the high-level waste(HLW) as nitrates will be converted to the solid particles by a sol-gel technique with a high yield. The gel particle is formed as a mixture of the actinide oxides and carbon, which is converted to mononitride by carbothermic reduction in a nitrogen atmosphere. The particles of uranium mononitride, UN, have been fabricated in order to study the fabrication process.

The feed solution with a C/U ratio of 2.75 was prepared by mixing uranium nitrate solution, carbon powder, hexamethylenetetramine(HMTA) and urea. The HMTA decomposes to form ammonia on heating to about 360K. The liquid droplets then turns into gel particles. The gel particles were washed, dried and calcined at 753K. The oxide with carbon was converted to nitride by first heating to 1,773K in N_2. Further heating at 1,673K in N_2-8%H_2 promoted the reaction of UO_2 with carbon through HCN and the removal of the residual carbon. Photo. 1 shows the UN particles thus produced. High purity UN particles with 660 ppm oxygen and 30 ppm carbon have been fabricated. Further efforts are being made:

(1)Controlling the particle density.

(2)Fabricating the mixed nitride of uranium and rare earth elements. The latters are substitutes for minor actinide.

2.2 Fabrication of nitride fuel pellets

Pellets-type uranium-plutonium mixed nitride, (U,Pu)N, has been fabricated by a conventional route with carbothermic reduction of the dioxides with graphite, followed by ball-milling, compacting and sintering[4,5]. The carbothermic reduction is carried out at about 1,920K in H_2-8%N_2 mixed gas flowing for about 36 ks.

For irradiation tests, the thermally stable pellets were fabricated by introducing relatively large pores in dense fuel matrix by use of pore former[5] so that pellet density could be kept about 85 %TD. Fine nitride powder was used to obtain dense matrix because of its poor sintering characteristics. Sintering was performed at about 2,000K for 18 ks in an Ar-8%H_2 atmosphere followed by the heat treatment at 1,730K in N_2-8%H_2 mixed gas stream. The microstructure of the pellet is shown in Photo. 2, where black circles were pores introduced by pore former.

3. Fuel Property Measurements

The lattice parameters of the quasi-binary systems of plutonium mononitride, PuN, with UN and neptunium mononitride, NpN, were determined by X-ray diffraction analysis of the solid solutions. It is found that the NpN-PuN system shows completely mutual solubility over the whole range of compositions, similarly to the UN-PuN systems[6]. It is also indicated that its lattice parameter deviates positively from the Vegard's law, especially in the PuN-rich compositions as well as that of the system of UN-PuN. The deviation from the Vegard's law could be explained by the behavior of 5f electron.

Knudsen-effusion mass-spectrometric experiments of NpN and the solid solutions of NpN and PuN were carried out. It was reported from the preliminary experiments of NpN that NpN showed the congruent evaporation[3], but further studies have led to the conclusion that the NpN might be considered to decompose into liquid neptunium and nitrogen gas as follows;

$$NpN(s) = Np(l) + 1/2N_2(g)$$
$$Np(l) = Np(g)$$

The standard free energy of formation of NpN estimated from the data can be represented by the following equation[7];

$$\Delta Gf = -295{,}870 + 91T(J/mol).$$

With regard to the vaporization behavior of the solid solutions of NpN and PuN, Np(g) and Pu(g) were detected as predominant gas species. The temperature dependence of the partial pressures of Np(g) suggested the precipitation of liquid neptunium. On the other hand, the temperature dependence of the pressures of Pu(g) was rather complicated; at higher temperatures, it showed a similar behavior with PuN, but, at lower temperatures, the precipitation of liquid plutonium might be suggested.

The thermal diffusivities of actinide nitrides have been measured by use of a laser-flash method for estimating the thermal conductivities. The results on the thermal conductivities of UN, PuN, NpN and the solid solutions of UN-PuN were reported in earlier papers[8,9]. It is confirmed from the estimated values that the thermal conductivity of actinide mononitrides decreases with the atomic number of heavy metals as shown in Fig. 1. The thermal conductivities of the solid solutions of NpN and PuN were also determined. The solid solutions have a similar temperature dependence with NpN and PuN and show intermediate values between those of NpN and PuN.

The details of the properties of the solid solutions of NpN and PuN will be presented at this meeting[10].

4. Irradiation Behavior

Four encapsulated fuel pins of uranium-plutonium mixed nitride, $(U_{0.8}Pu_{0.2})N$, were irradiated at JMTR up to the maximum burn-up of 5.5%FIMA at maximum heating rates of 650 - 730 W/cm as shown in Fig. 2. Thermal stable nitride pellets were fabricated for the tests as described above. The typical characteristics of fuel pins are shown in Table 1. No pin failure was observed in all the cases. The preliminary results of FP gas release from the nitride fuel are plotted in Fig. 3 as a function of burn-up, together with those of mixed carbide fuel irradiated in JMTR and Japan Research Reactor-2 (JRR-2). It is obvious that nitride fuel shows very low fission gas release; 2~3 % at the burn-ups of 4~5%FIMA because of its advantageous thermal characteristics and also the stabilization of fuel matrix by introducing the thermal stable pellets. Furthermore, it is confirmed that the maximum diameter increase rate of the fuel pins was about 1 %/%FIMA or less and the fission gas retained in fuel matrix does not significantly accelerate gas swelling of nitride fuel, at least up to the burn-up of 5.5%FIMA.

At present, two pins of mixed nitride fuel are under irradiation in the experimental fast reactor 「JOYO」 for a target burn-up of 4.5%FIMA as a joint research with JAERI and Power Reactor and Nuclear Fuel Development Cooperation (PNC).

5. Reprocessing Technology

5.1 Estimation of process and mass balance evaluation

The process of the molten-salt electrorefining of nitride fuel is similar to that of metal fuel: nitride fuel is anodically dissolved and the actinide metals are deposited on the dual cathodes[11], which consists of a solid cathode for the recovery of U and a liquid-Cd cathode for that of TRUs. Simulation calculations for nitride FBR fuel were made with use of the PALEO code to determine the amounts of actinides recovered in the electrorefier and to estimate decontamination factors of fission products. The PALEO code, which is similar to the TRAIL code[12], calculates electrochemical behavior for Pu or U using diffusion layer model. In this calculation, the basic data such as standard potentials of actinides and lanthanides were taken from Ref. 13, and rare earth elements were represented by Ce which is one of the most difficult elements to be separated from actinides. It was found from preliminary calculation that the Ce concentration in the salt should be lower than 4.0wt% to keep the decontamination factor of about 5.

Equilibrium concentrations of main elements in LiCl-KCl eutectic melt were set to be 7.0wt% for Pu, 4.0wt% for U, 0.19wt% for minor actinides(Am) and 4.0wt% for rare earth(Ce) so that the Pu concentration in the output actinides from the electrorefining process might be almost same as that in the input actinides. The anode and cathode potentials were controlled to be -0.50V and -1.4V versus Ag/0.1wt%AgCl during electrorefining. As a result of the simulation calculations, the time dependent concentaration of each element in the salt is shown in Fig.4. At the first stage, Pu, Ce, Am and then U are well resolved, and U is deposited on the solid cathode. After exchanging the cathodes, Pu, U, Ce and Am are deposited on the liquid Cd cathode. The process time is about 7 hours for the first stage, and about 2.5 hours for the second stage.

In order to keep the rare earth concentration in salt around 4.0wt%, some amount of the salt(6.7% of the salt) have to be removed at each batch from the electrorefining vessel. The removed salt first goes through a stripping step with Cd-Li, and then an extraction step with Cd-U. The process calculation was made using the distribution coefficients(wt% in salt/wt% in Cd)[14]; 1 for U, 2 for Pu, 4 for minor actinides, 40 for rare earths, and 1,000 for alkali and halogen. Considering the Pu recovery rate and the rare earth concentration in Pu, the values of 1 for U distribution coefficient in the stripping process and 3 for Cd/salt ratio in extraction process were selected. The stripping and extraction steps remove almost all the actinide from the salt to Cd and leave about 72% of the rare earth in the spent salt. Actinides recovered in the Cd solution are returned to the electrorefiner.

Table 2 summarizes the mass flow in the electrorefing and salt treatment processes. The annual processing capacity is set to be 44 ton-HMeq(heavy metal equivalent) which corresponds to the amount of spent fuels from 4GWe nitride FBR. Average burnup of the discharged fuels is 100GWd/ton for core fuels and 12 GWd/ton for blanket fuels. About 220kg-HMeq per day are processed when the annual working day is assumed to be 200 days. Witout considering the process loss, 99.45% of U and 99.95% of Pu can be recovered after adding those from the salt process.

5.2 Electrolysis of actinide nitrides

Anodic dissolution of UN in the eutectic melts of LiCl and KCl has been studied to provide a basis for the feasibility study of the electrorefining of irradiated nitride fuels[13]. The threshold potential of the anodic dissolution of UN was observed as shown in Fig. 5, where the working electrode was first cathodically polarized to -2.40 V and then potential was raised from the rest potential, about -1.6 V, to -0.2 V. It was consistently explained with the thermochemical

database of pure substances. The anodic dissolution of UN as U^{3+} into LiCl-KCl begins at the standard electrode potential of E: = -0.82 V referring to the equilibrium Ag/Ag^{+}. It is considered that the threshold potential is determined by the formation of solid UCl_3 on UN. At present the possibility of direct nitriding of actinides in molten Cd-alloys is investigated.

Laboratory-scale electrorefiners for handling NpN and PuN have been installed in gloveboxes of 5 m^3 in which purified argon gas is circulated at a rate of about 50m^3/hr and the concentrations of oxygen and water impurities are kept less than 1 ppm. The photograph of the argon gas atmosphere gloveboxes is shown in Photo. 3. The experiments are planned to start in 1996.

6. Summary

The present status of the research and development of nitride fuel cycle for TRU burning at JAERI is described. The fabrication technology of nitride fuel particles by a sol-gel method has been investigated and UN particles with high purity have been successfully fabricated, beside that pellet-type mixed nitride fuel by an conventional route. The properties of NpN-PuN solid solutions such as lattice parameter, thermal conductivity and evaporation behavior were determined. From the irradiation tests of mixed nitride fuel pins at JMTR, it is confirmed that nitride pellets shows very low FP gas release as expected. The pyroprocess for nitride fuel was estimated and the mass balance in the process was described.

References

[1] H. Blank, J. Less-Comm. Met., 121 (1985) 583.
[2] T. Mukaiyama, T. Ogawa and Y. Gunji, IAEA P-T Tech. Committee Mtg., Vienna, Nov. 29 - Dec. 2, 1993.
[3] Y. Suzuki, T. Ogawa, M. Handa, Proc. on 3rd OECD/NEA Int. Mtg on Actinide and Fission Product Partitioning and Transmutation, (1994) p.250.
[4] Y. Arai, S. Fukushima, K. Shiozawa and M. Handa, J. Nucl Mater., 168(1989)280.
[5] Y. Suzuki, Y. Arai, and T. Sasayama, J. Nucl. Mater., 115(1983)331.
[6] Y.Suzuki, A.Maeda, Y.Arai and T.Ohmichi, J. Nucl. Mater., 188(1992)239.
[7] K.Nakajima, Y.Arai and Y.Suzuki, 9th Int. Symp. on Thermodynamics of Nuclear Materials, STNM-9, Osaka, Aug.26-30, 1996.
[8] Y.Arai, Y.Suzuki, T.Iwai and T.Ohmichi, J. Nucl. Mater., 195(1992)37.
[9] Y.Arai, Y.Okamoto and Y.Suzuki, J. Nucl. Mater., 211(1994)248.
[10] Y.Arai, K.Nakajima, Y.Suzuki, to be presented in this meeting.
[11] J.J.Laidler, J.E.Battles, W.E.Miller and E.C.Gay, Proc. on GLOBAL'93 (1993) p.1061.
[12] T.Kobayashi and T.Tokiwai, J.Alloys and Compounds, 197 (1993) 7.
[13] F.Kobayashi, T.Ogawa, M.Akabori and Y.Kato, J. Am. Ceram. Soc., 78(1995)279-2281.
[14] L.S.Chow, J.K.Basco, J.P.Ackerman and T.R.Johnson, Proc. on GLOBAL'93 (1993) p.1080.

List of table, figure and photograph

Table 1 Typical characteristics of nitride fuel pins irradiated at JMTR

Fuel pin		
Pin length	(mm)	250
Fuel length	(mm)	100
Outer diameter	(mm)	9.40
Cladding material		20%CWSUS316/Ferritic SUS
Cladding thickness	(mm)	0.51
Inter diameter	(mm)	8.38
Smear density	(%TD)	80
Fuel pellet		
Material		(U,Pu)N
Pu/(U+Pu)		0.20
Pellet diameter	(mm)	08.18 - 8.23
Pellet density	(%TD)	83 - 86
Pellet/cladding diameter gap	(mm)	0.15 - 0.20
Bonding material		He

Table 2 Mass flow in the electrorefining and salt treatment process

(1GWe x 4 FBRs equivalent) (kg/day)

Element	(a)	(b)	(c)	(d)	(e)
U	200.40	200.40		180.58	22.71
Pu	22.72	22.72			22.71
MA	0.88	0.88			0.88
ALM	1.32	1.32			
RE	2.61	2.61			0.52
NM	5.52	5.52			
HL	0.14	0.14			
$^{15}N_2$	14.16	14.16			
VFP	1.48		1.48		
Na	16.88		16.88		
SM	800.00	52.00	748.00		

Element	(f)	(g)	(h)	(i)	(j)
U	2.91	2.65	0.26	3.15	1.49
Pu	5.10	4.25	0.85	0.835	0.015
MA	0.138	0.099	0.039	0.038	0.001
ALM	1.32	0.01	1.31		1.31
RE	2.91	0.58	2.33	0.24	2.09
HL	0.14		0.14		0.14

MA : Minor Actinide RE : Rare Earth NM : Noble Metal HL : Halogen
ALM : Alkali VFP : Vaporous FP SM : Structural Material

(a) - (j) : See bellow

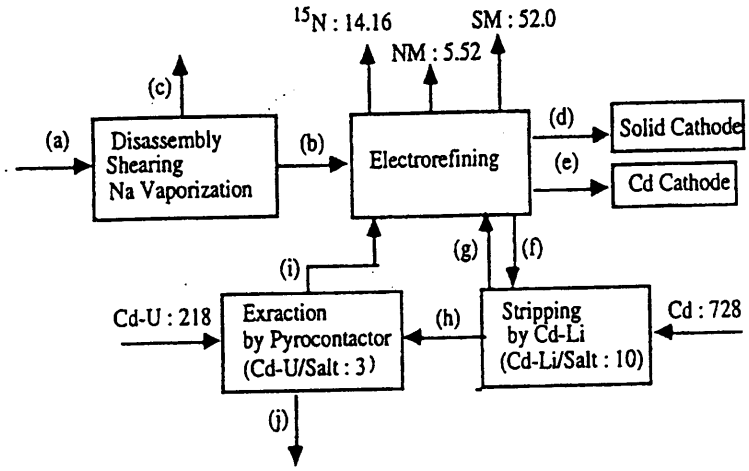

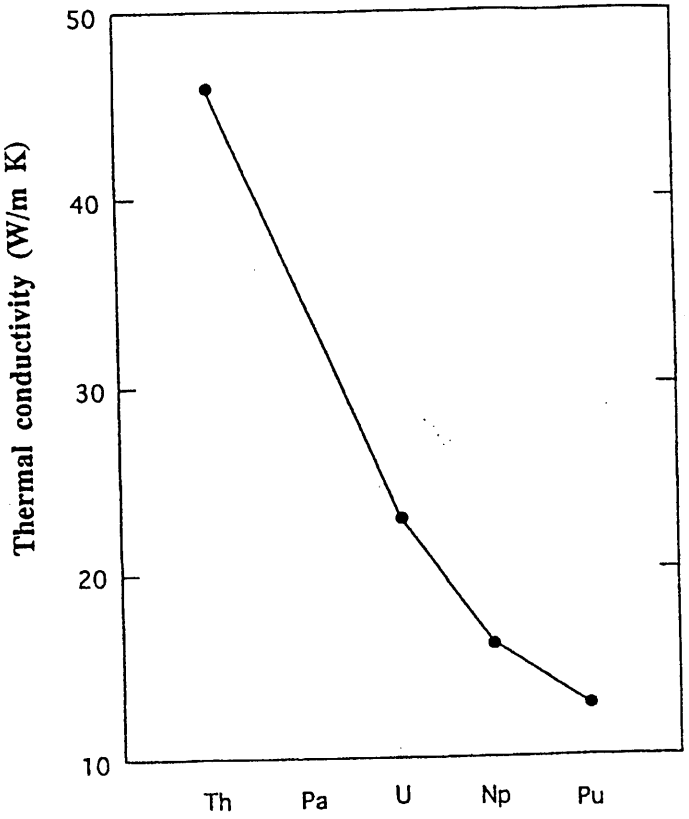

Fig. 1 Thermal conductivity of actinide mononitrides

Test No.	Reactor	No. of pins	Dia. (mm)	Linear power (kW/m)	Burnup (%FIMA)
1	JMTR	2	9.4	65	4.1
2	JMTR	2	9.4	73	5.5
3	JOYO*	2	8.5	(80)	(4.5)

'87 '89 '91 '93 '95 '97 '99

* Under collaboration research program with PNC

Irradiation —— PIE

Fig. 2 Irradiation program of nitride fuel

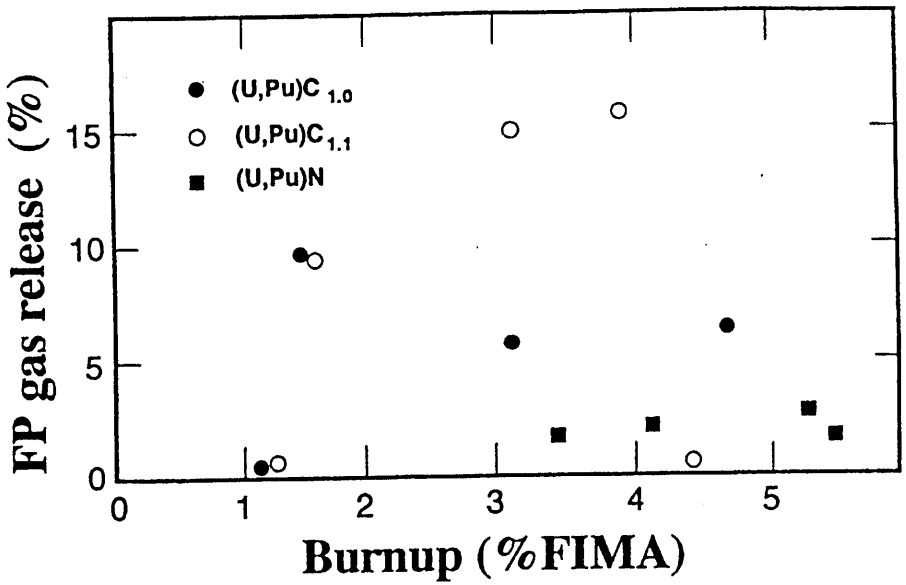

Fig. 3 FP gas release from carbide and nitride fuels irradiated in JRR-2 and JMTR

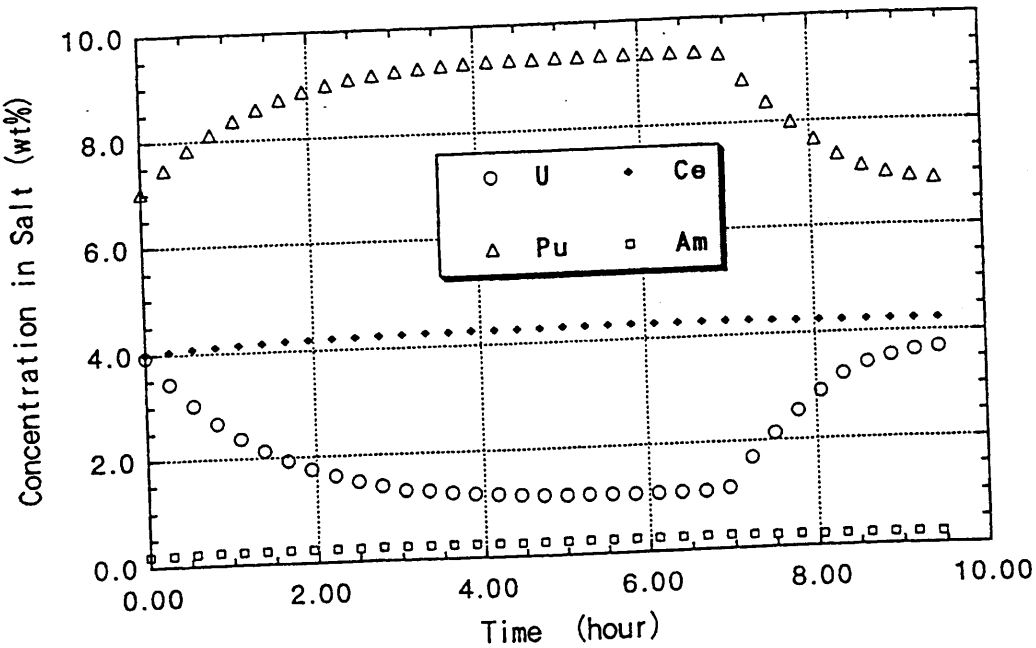

Fig. 4 Element concentration in salt at electrorefining of nitride fuel (U/Pu/Am/Ce=4.0/7.0/0.19/4.0),

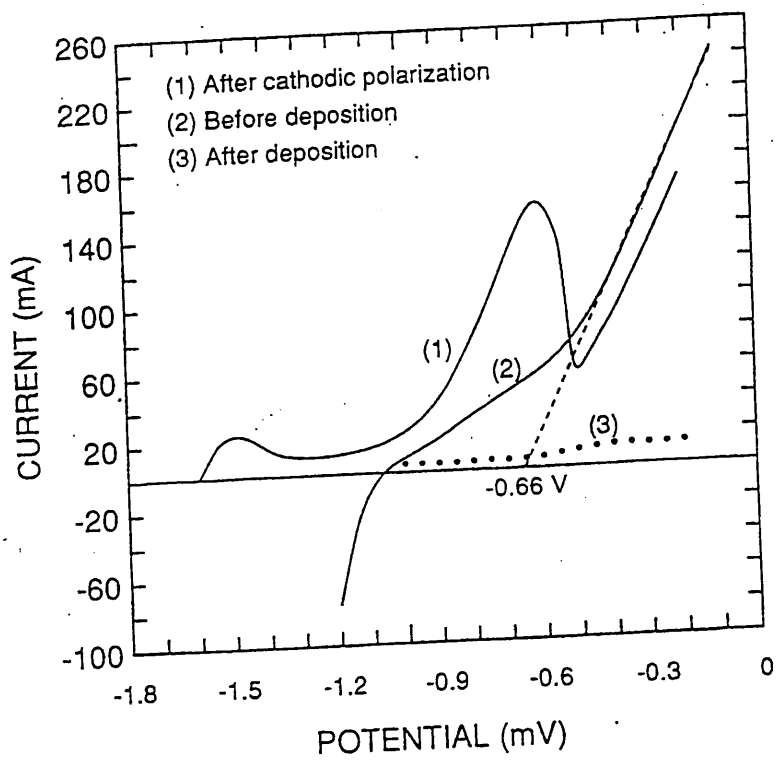

Fig. 5 Results of potentiodynamic measurements of UN

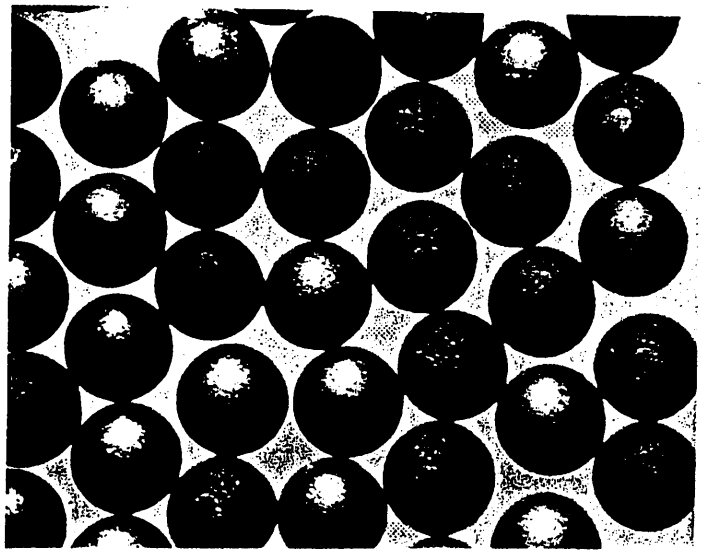

Photo.1 UN paricles fabricated by sol-gel process followed by carbothermic synthesis.

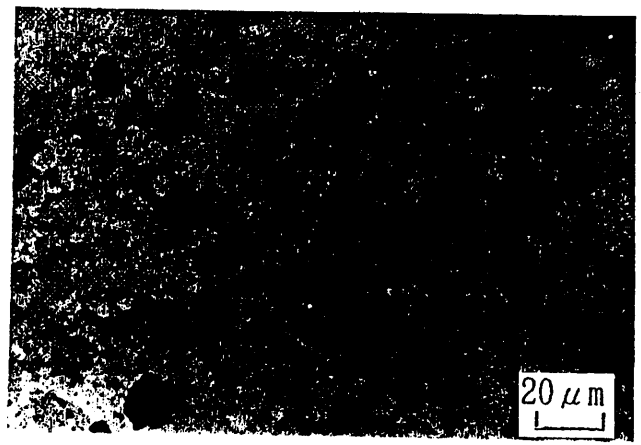

Photo.2 Microstructure of thermal stable nitride pellet

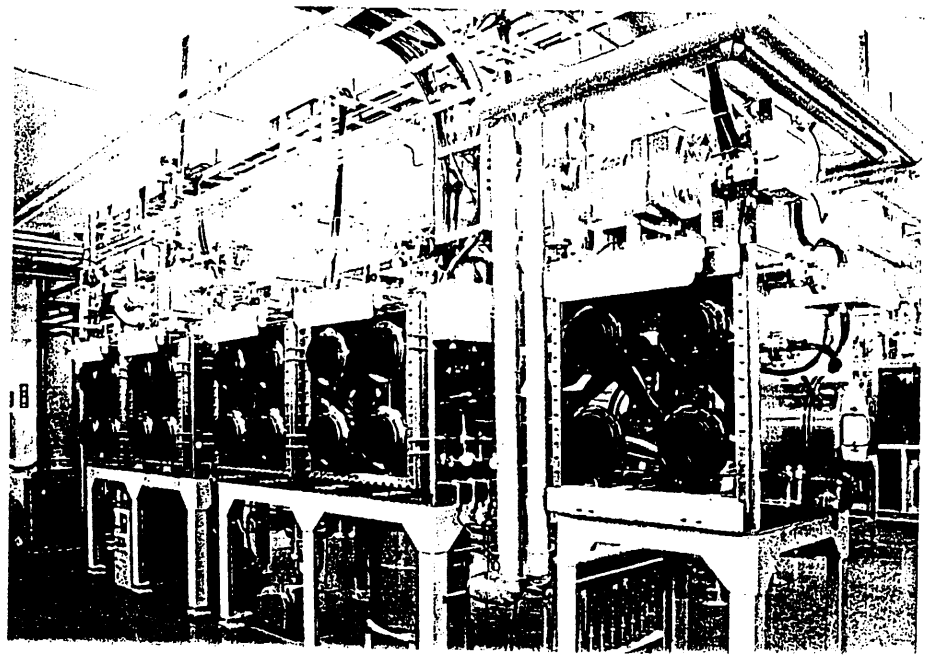

Photo.3 Appearance of gloveboxes in which electrorefiners for PuN and NpN are installed

CONSTRAINTS OF THE FABRICATION OF AMERICIUM OXIDE TARGETS

A. Renard, A. La Fuente, S. Pilate (BELGONUCLEAIRE, Brussels)
A. Harislur, M. Mouney, M. Rome (ELECTRICITE DE FRANCE, Paris & Lyon)

Abstract

If a special fabrication chain is devoted to prepare AmO_2 target pins in a MOX fuel fabrication plant, the dose rates will be considerably increased with respect to the present MOX (UO_2, PuO_2) fuel pin fabrication practice.

This memo shows results of orientation calculations, as recently performed at BN, with the close follow-up by EDF.

The accent is stressed on the validation of the calculational route via the evaluation of measurements available.

1. INTRODUCTION

After plutonium, americium is the second most important transuranium radio-isotope for what concerns the long-term waste radiotoxicity. With its half-life of 433 years, americium 241 contributes to a large part of the activity and toxicity of waste after 1000 years, while its decay raises the content in Np237. Americium 243 is less important as its half-life is 7380 years.

Ways to reduce the amount of americium by transmutation via reactor irradiation, either in pressurised water reactors (PWR) or in fast reactors, are thus under investigation.

At BELGONUCLEAIRE, the merits of homogeneously spreading americium oxide, supposed recovered at reprocessing, into the mixed oxide (MOX) fuel, have first been identified. Core physics calculations were first run to define the range of Am mixing fractions and Pu enrichments which would be required for such fuels in PWRs. Then, the radioprotection implications of manufacturing these special fuels have been determined from an extrapolation of the fuel fabrication conditions in present MOX fuel plants like that of BELGONUCLEAIRE at Dessel (1).

The results of these investigations were published at the preceding OECD meeting in Cadarache (2) and later on in open conference (3).

The heterogeneous irradiation of Am in PWR is being considered in turn. Target fuel pins would contain AmO_2 with an inert material, like (Al_2 Mg O_4), transparent to neutrons. These pins could be inserted either in the bundle of MOX fuel assemblies, or in dedicated assemblies containing only target pins. A paper has presented solutions which seem acceptable from the point of view of reactor designers and operators (4) : they would allow to reduce the americium content by irradiation in a way which does not deteriorate reactor performances and safety.

What would be the burden of heterogeneous Am recycling on the MOX fuel fabrication plants ? This is the subject of current studies ; first results are presented in this paper. The accent is stressed on the validation of the results obtained.

ASSUMPTIONS ON OXIDE POWDERS AND TARGET PINS

The first assumption is that the MOX fuel fabrication plant would have a chain dedicated to AmO_2 fuel, in parallel to the usual PuO_2-UO_2 chain.
The front-end and back-end could stay in common, i.e. :

- it is imagined to receive AmO2 powders from the reprocessors in the same packing and in similar storage vaults than for PuO_2-UO_2 at present,

- bundles of target fuel pins could be directed to assembly mounting halls, shipped in containers suited to on-site transportation.

In practice, for the sake of comparative calculations, the storage vault currently used has been supposed to contain pure AmO_2 powder instead of pure PuO_2 powder.

The incoming Am contains the following isotopic fractions : Am 241/242/243 = 62.4 % / 0.3 % / 37.3 %.

They are typical of americium fully recovered (with a 99 % yield) from the PWR fuel discharged after a burnup of 44 Gwd/t, 5 years after discharge. The isotopic Pu composition retained for comparison is :

Pu 238 / 239 / 240 / 241 /242/ Am 241 = 2.4 / 53.4 / 23.6 / 12.3 / 7.1 / 1.2 %

The target pin is supposed to contain 20 % AmO_2 diluted with Al_2O_3. This relatively low AmO_2 content has been found optimal in view of a large reduction factor by irradiation, of 90 % for Am241 and 50 % for Am242 (4). The MOX pin retained as a reference for comparison contains 7.8 % Pu, i.e. an enrichment equivalent to 3.7 % U235 in PWRs, which becomes typical of MOX fuel nowadays.

The AmO_2 dedicated assembly to be constituted would consist, as the standard 900-MWe PWR assembly, of 264 active pins and 25 guide-tubes, arranged according to a 17 x 17 square lattice ; the active height is 3.66 m.

COMPUTER CODES USED

Three-dimensional dose-rate calculations have been performed using the codes QAD-CGGP (6) for gamma-rays and MCNP-4A (7) for neutrons. The radioactive sources have been established using ORIGEN-2 (8), taking into account irradiation history and the hypotheses given above.

PRELIMINARY COMPARATIVE RESULTS

- Storage of powders

Figure 1 shows a sketch of the storage vaults ; each vault can comprise a maximum of 5 cans containing each 3 kg oxide powders. The dose rates are calculated at 30 cm distance from the shielded doors.

Table I gives dose rates calculated for the presence of PuO_2 or AmO_2 powders, respectively, and their ratios.

For gamma-rays, the rise from Puo_2 to AmO_2 is by a factor 185 ; for neutrons this is by a factor 3.

To reduce the dose rates to the same levels needs the addition of 7 cm lead thickness to the shielded door.

TABLE I
Powder Storage Vaults
Dose rates at 30 cm distance from the door (mSv/h)

	Gamma dose	Neutron dose	Total
PuO_2	0.015	0.019	0.034
AmO_2	2.77	0.060	2.83
Ratio	185	3	82

- Handling and transportation of pins

A transfer of 200 pins is considered towards the assembly mounting hall, inside of a steel canister of a square section by 21 x 21 cm and a 5 mm thickness.

The IAEA rules for transportation of radioactive materials limit the dose rates to 2 mSv/h on surface and 0.1 mSv/h at 2 m distance. These limits have only an indicative value, as the considered transfer remains inside of the site, and is not a public road transportation.

Table II gives dose rates calculated at 1 m distance, for 200 pins either corresponding to the reference MOX conditions, or to AmO_2 target pins.

For gamma-rays, the rise from MOX to AmO_2 is by a factor 2780 : for neutrons it is about 7. To reduce the dose rates to the same levels needs typically the addition of about 4 cm lead and 4 cm resin to the shielding, and to transport only half of the pins, i.e. 100, at the same time.

TABLE II
Transfer Canister for Pin Bundles
Dose rates at 1 m distance (mSv/h)

	Gamma dose	Neutron dose	Total
MOX pins	0.097	0.135	0.232
AmO_2 target pins	270	0.94	271
ratio	2.780	7	1170

VALIDATION OF THE COMPARISONS

Much work has been focused on the validation of the results, especially because the extrapolation to be done from the present MOX fuel fabrication experience is huge.

Some aspects of this validation are detailed hereafter.

1. Dose from storage of MOX fuel

The dose rate has been measured at BELGONUCLEAIRE Dessel in front of the door of a storage vault containing 5 PuO_2 powder cans (double boxes), and compared to calculations.

The measurement was made at 63 mm distance from the external face of the door, which is made of sandwich layers of stainless steel, lead, boron containing glass, polythene and cadmium, see Figure 1.

Each of the 5 cans contained about 3 kg of PuO_2, with the following isotope composition :

Pu238 / 239 / 240 / 241 / 242 / Am241 = 1.32 / 57.38 / 24.15 / 6.11 / 5.11 / 5.93 %.

This measurement was selected for calibration of the methods, as it refers to an aged plutonium with as much as nearly 6 % Am241 / Pu.

The comparison between calculation and measurement is given in Table III below.

TABLE III
Calibration of Methods
1. Storage of aged PuO_2

Dose Rates (μSv/h)	Calculated	Measured
from gamma-rays	22.5	23*
from neutrons	33	29

* 23 : is the average of 5 measurements ; the extreme values were 23 ± 7 ; background was discounted.

The differences between calculation and measurement are quite acceptable.

Similar measurements were also made with the door open ; the differences (C-E)/E were about 20 % for gamma-rays, what is also acceptable. For neutrons, the calculations overestimate the dose as above.

Note that with this type of Pu, Am241 contributed to about 50 % of the gamma dose.

2. Dose from a transport container

The case of the transport of 2 fresh MOX assemblies into a specific container with 2 positions has been considered. Results of measurements are available for 3 m-long MOX assemblies of 14 x 14 pins, with an average Pu enrichment of 5.3 %

A double steel wall, 4 cm-thick in total, comprises a 4-cm thick resin layer.

Table IV gives the comparison of calculated and measured dose rates on the surface of the container.

TABLE IV
Calibration of Methods
2. Transport container (MOX)

Dose Rates (μSv/h)	Calculated	Measured
from gamma-rays	28.8	32
from neutrons	241	208

The comparison is satisfactory. The neutron calculation, by Monte-Carlo method with a statistical uncertainty of 3 %, overestimates the measurement by 15 % ; fluctuations of the resin composition could explain this deviation.

3. Dose from a SUPERFACT pin

The irradiation experiment SUPERFACT has been conducted in the fast reactor PHENIX, up to a burnup of 5 %. The capsule contained in particular special pins loaded with americium, which had been fabricated at TUI Karlsruhe, see (5).

Pin SF No.14 contained mixed oxide, the metal being 20 % Am241, 20 % Np237 and 60 % depleted uranium. The radial pin dimensions were typical of PHENIX : 5.42 mm pellet o.d., 6.55 mm cladding o.d.

For this fresh pin, dose rates have been measured at TUI. The measurement retained for this calibration is at a distance of 1 m from the pin, without any additional shielding. According to TUI (5), their calculation reproduces well the measurement.

Table V below compares two sets of calculation results, the one from TUI (5), and the other one with the BELGONUCLEAIRE methods, described above.

Both calculated routes have been applied in parallel to a standard PHENIX pin, of same radial geometry, containing mixed oxide UO_2-PuO_2 with a Pu enrichment of 25 % and a Pu isotopic composition of :

Pu238 / 239 / 240 / 241 / 242 / Am241 : 1.3 / 60.4 / 23.4 / 9.9 / 4.5 / 0.5 %

TABLE V

Calibration of Methods

3. SUPERFACT pin with Am

Dose Rates (mSv/h)	Calculated at TUI	Recalculated
SUPERFACT pin 14 :		
- from gamma-rays :	0.25 [1)]	0.33
- from neutrons :	-[2)]	0.00057
Standard PHENIX pin :		
- from gamma-rays :	0.0065	0.0068
- from neutrons :	0.00018	0.00028

[1)] measured : 0.26

[2)] no measurement quoted

For the SF14 pin, Table V shows an overestimate of about 30 % for the gamma-ray dose. While our calculations are showed to be conservative, the difference could be associated with the gamma source spectrum found with ORIGEN2 (TUI used a source from the KFK improved version KORIGEN).

For neutrons, the values for the PHENIX pin shows a difference by about +50 % ; the dose due to neutrons is anyhow much smaller than the gamma dose.

From the PHENIX pin to the SF14 pin, the gamma dose increases by a factor 40 to 50, and the neutron dose by a factor 2.

These cross-checks may be considered satisfactory for the sake of orientation calculations.

PROVISIONAL CONCLUSIONS

The fabrication of AmO_2 target pins in a MOX fabrication plant indicate that, with respect to the dose rates experienced in present MOX (UO_2 PuO_2) fuel fabrication, the dose rates emanating from AmO_2 powders, from target AmO_2 pins and from bundles of such pins, would be significantly higher if no re-inforced shielding was applied. The raise of the dose rates would reach factors like :

80 in front of the shielded doors of the oxide powder storage vaults

50 from a single Am target pin compared to a standard fast reactor pin geometry,

2800 from a canister transferring 200 pins to the mounting hall.

The increase in shielding thickness necessary to lower dose rates to the levels currently observed in MOX fabrication, has been determined by calculation.

It appears that the fabrication of AmO_2 target pins should preferably be done in shielded hot cells.

As the americium mass recoverable from PWR irradiated fuel (after 5 years)is about 6 % of the plutonium mass, and considering the assumption made here (MOX pins with 7.8 % Pu, target pins with 20 % AmO_2), the production of Am target pins would amount to about 1/50 of the MOX pins.

The transportation of dedicated AmO_2 assemblies obviously needs a re-inforced shielding on the containers. The practicability of such transportation is being studied in further details.

A large effort has been spent to check the validity of the calculations. To that aim, 3 important steps of the fabrication chain have been covered by experimental validation :

- the storage of incoming powders for which measurements are obtained from BN/Dessel for relatively aged PuO_2 batches,

- the transport container, for which measurements are obtained for current MOX assemblies,

- and the constitution of single pins containing 20 % AmO_2, for which TUI Karlsruhe had measured and calculated dose rates.

The comparisons made bring confidence in the validity of the predictions.

REFERENCES

[1] D. HAAS, A. VANDERGHEYNST & J. van VLIET (BELGONUCLEAIRE)
R. LORENZELLI & J.L. NIGON (COGEMA)
Mixed-Oxide Fuel Fabrication Technology and Experience at the BELGONUCLEAIRE and CFCa Plants and Further Developments for the MELOX Plant
Nuclear Technology, Vol. 106 (April 1994)

[2] T. MALDAGUE, S. PILATE, A.F. RENARD
Impact of Plutonium and Americium Recycling in PWR on MOX Fuel Fabrication
Proc. of the 3rd International Information Exchange Meeting on Actinide and Fission Product Partitioning and Transmutation, Cadarache, France, December 12-14, 1994.
OECD/NEA

[3] A. RENARD, S.PILATE, T. MALDAGUE, A. LA FUENTE, G. EVRARD
Implications of Plutonium and Americium Recycling on MOX Fuel Fabrication
GLOBAL'95, International Conference on Evaluation of Emerging Nuclear Fuel Cycle Systems, Versailles, France (September 1995).

[4] T. MALDAGUE, S. PILATE, A. RENARD (BELGONUCLEAIRE)
A. HARISLUR, H. MOUNEY, M. ROME (ELECTRICITE DE FRANCE)
Core Physics Aspects and Possible Loadings for Actinide Recycling in Light Water Reactors
GLOBAL'95, International Conference on Evaluation of Emerging Nuclear Fuel Cycle Systems, Versailles, France (September 1995).

[5] G. NICOLAOU & al.
Experimental Nuclear Data in Relation to Irradiation Experiments of Minor Actinide Targets in Fast Reactors
GLOBAL'95, International Conference on Evaluation of Emerging Nuclear Fuel Cycle Systems, Versailles, France (September 1995).

[6] QAD-CGGP, a Combinatorial Geometry Version of QAD-P5A, a Point Kernel Code System for Neutron and Gamma-Ray Shielding Calculations using the GP Buildup Factor
Contributed by JAERI and ORNL - CCC-493 (1987)

[7] J. BRIESMEISTER (Editor)
MCNP, a General Monte Carlo Code for Neutron and Photon Transport
LA-7396-M (September 1986, revised April 1991)

[8] A.G. CROFF
A User's Manual for the ORIGEN2 Computer Code
ORNL/TM 7175 (July 1980)

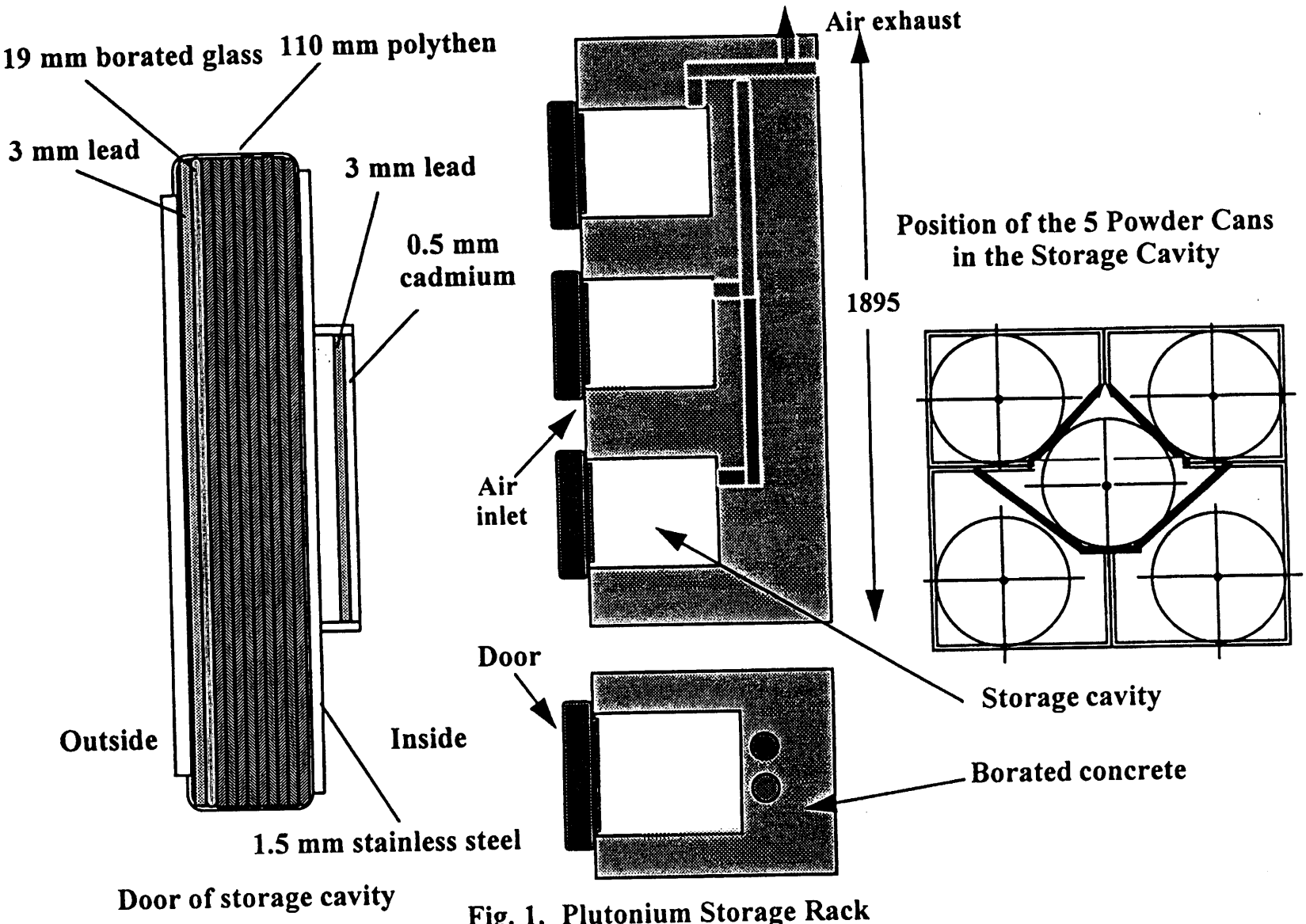

Fig. 1. Plutonium Storage Rack